In-vivo imaging of root growth in response to localized mechanical stress

Leah Eitelberg

Master thesis • 30 credits
Swedish University of Agricultural Sciences, SLU
Faculty of Natural Resources and Agricultural Sciences/Department of Soil and Environment
Soil Water and Environment Programme – 120 credits
Series title, Part number • 2022:10
Uppsala, 2022

In-vivo imaging of root growth in response to localized mechanical stress

Leah Eitelberg

Supervisor: Tino Colombi, Department of Soil and Environment
Assistant supervisor: Thomas Keller, Department of Soil and Environment
Examiner: Björn Lindahl, Department of Soil and Environment

Credits: 30 hp
Level: Second level, A2E
Course title: Master thesis in Soil science, A2E – Soil Water and Environment Programe
Course code: EX0880
Programme/education: Soil Water and Environment, 120 ECTS
Course coordinating dept: Department of Soil and Environment
Place of publication: Uppsala, Sweden
Year of publication: 2022

Part number: 2022:10

Keywords: kinematics analysis, time-lapse imaging, root growth rate, root curvature, soil heterogenety, local mechanical stress

Swedish University of Agricultural Sciences
Faculty of Natural Resources and Agricultural Sciences
Department of Soil and Environment

Abstract

By taking up nutrients and water, root growth has an important influence on plant growth and productivity. Thereby, root growth is influenced by its surrounding soil conditions, which vary spatially even on a small scale. Hence, different parts of the root system are exposed to different penetration resistances in the soil. As root cells are connected by their cell walls, information about growth conditions can be transferred throughout the root system, which is why roots can react to the soil conditions of their neighbouring roots.

By doing in-vivo measurements in a hydroponic system, this study investigated the responses of unimpeded roots to local mechanical stress of their neighbouring roots. To do so, the primary or seminal roots were exposed to vertical or horizontal obstacles. Using a time-lapse imaging system under infra-red light in combination with particle image velocimetry the underlying processes of root growth, such as the growth direction, the growth rate, the cell elongation rate, and the growth zone length were quantified.

In this study, the primary and seminal roots showed contrasting responses of root growth rate and root growth direction. While the primary roots did not response to a restriction in growth of the seminal roots, seminal roots reacted to the applied stress in the same way as the impeded roots, even if the stress did not occur in their environment. In the case, where the roots found a way to work around the anticipated stress, they compensated for the impaired root with an increase in growth rate.

The fact, that the primary root did not show this response, might be due to their different functions in the root system. Furthermore, the relative root growth rate was stronger associated with the relative length of growth zone than with the relative elemental elongation rate. Nevertheless, the elemental elongation rate might be the driver for short-term adjustments.

Keywords: kinematics analysis, time-lapse imaging, root growth rate, root curvature, soil heterogeneity, local mechanical stress

Table of contents

List of tables

List of figures

Abbreviations

Abs	Absolute values
EERmax	Maximal elemental elongation rate, proxy for cell elongation
LSD	Least significant difference test
PIV	Particle Image Velocimetry
PH	Treatment, where the primary root was restricted horizontally
Rel	Relative values
SH	Treatment, where the seminal root was restricted horizontally
SV	Treatment, where the seminal root was restricted vertically
xEER	Position along the central axis of the root at which the maximum EER occurs

Introduction

1.1 Why root growth is important and where it occurs

Roots play an important role for the plant growth and productivity (Ristova & Busch 2014). By anchoring the plant in the soil and taking up water and nutrients, they provide the plant with important resources. Thereby it is not only of importance, that nutrients are available, but it must also be ensured, that roots reach the nutrient pools in the soil. Hence, the value of the nutrients depends on their accessibility by the roots (Bray, 1954).

To access the nutrients, an unrestricted optimal distribution of the root system is needed. How roots spread in the soil is influenced by different stimuli, which is called tropism. (Bizet et al. 2016). Thereby gravitropism, hydrotropism, thermotropism and thigmotropism are the most extensively studied (Muthert et al. 2020), and describe the growth within the gravitational field (Chen et al. 1999), towards available water resources, in response to temperature (Muthert et al. 2020) and in response to touch signals (Monshausen & Gilroy 2009), respectively.

To reach these different resources, roots build up their tissue symmetrically around the longitudinal axis. Root growth takes place in the root apex, which is determined by the two processes: cell production and cell elongation (Youssef et al. 2018). Thereby, cells are produced in the root apical meristem, which lies behind the root cap (Jiang & Feldman 2005). In the cell division zone, they then divide to build up a sufficient pool of cells, which are then pushed basipetally into the elongation zone, where they stop dividing but start to elongate (Petricka et al. 2012; Bizet et al. 2015) (Fig. 1). The transition zone represents the border between the elongation zone and the root apical meristem, where cell division and cell elongation occur (Petricka et al. 2012; Bizet et al. 2015).

The driving force of the cell elongation is the turgor pressure, which is generated by water influx into the cells and leads to the growth pressure (Jin et al. 2013).

Youssef et al. (2018) found that the main driver of growth rate is the cell production rate. On the other hand, in short-term growth adjustments, the growth rate was integral to the root cell elongation rate (Youssef et al. 2018).

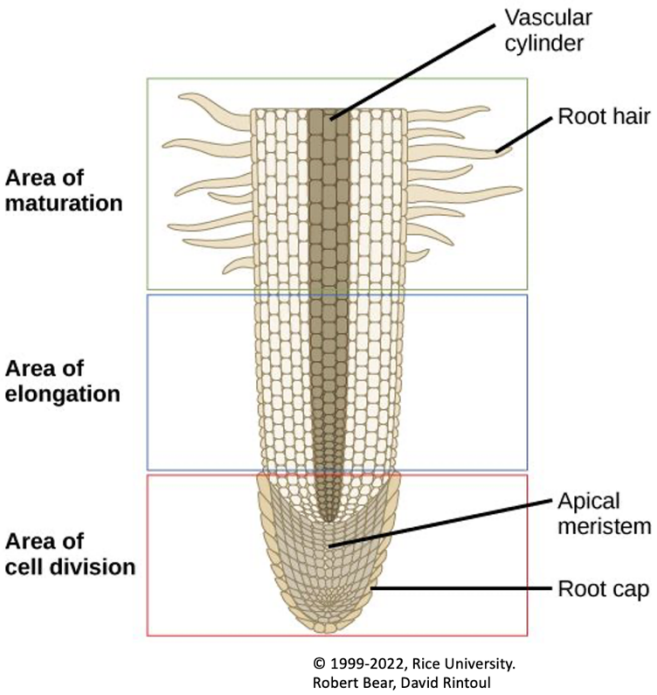

Figure 1: Schematic illustration of the root apical meristem, zone of cell division and zone of elongation in the growth zone by Robert Bear and David Rintoul, Rice University.

1.2 Roots grow in heterogenous soils

As most plants are anchored in the ground, root growth mainly takes place in soils (Voroney 2007). Therefore, roots and their growth behaviour are affected by the surrounding soil conditions. A good soil structure with a pronounced existing pore systems stimulates the root growth (Wang et al. 2020).

However, the growth behaviour of the root can also be affected negatively by the soil conditions (Barley 1970; Bengough et al. 2006; Rillig & Mummey 2006; Correa et al. 2019). Dry soil can increase the penetration resistance (He et al. 2017), while stones, large soil particles, dense aggregates and compacted soil represent physical obstacles for the roots (Bizet et al. 2016). To avoid hard soils, roots exploit parts with less resistance (Bizet et al. 2016; Wang et al. 2020). If the obstacle cannot be penetrated by the root, the root first starts to decrease its elemental elongation rate and growth zone and starts to change its growing direction by bending away to find another path (Jin et al. 2013; Bizet et al. 2016). The maximal bending of the root thereby takes place at the end of the growth zone (Bizet et al. 2016).

The occurrence of these unfavorable growing conditions is a result of complex processes that shape the soil structure. Different bedrocks and climate conditions thereby represent the initial conditions for different amounts of rock fragments (Sauer & Logsdon 2002), different wet-dry cycles (Jabro et al. 2014; He et al. 2017; Koebernick et al. 2017) and different soil management systems (Wang et al. 2020). Those processes and conditions in turn influences the porosity of the soil, which is important for the water storage capacity and infiltration rate (Lipiec et al. 2006), hence the soil strength and penetration resistance (Martino & Shaykewich 1994).

These different conditions and processes lead to a spatial soil heterogeneity, which also makes the resource availability and accessibility vary spatially and temporally (Clark et al. 2003; Hodge et al. 2009). This high spatial and temporal variability occurs on different scales, including the scale relevant to plant roots (Hodge et al. 2009). Therefore, it is important to understand the responses of roots to soil heterogeneities to establish root systems that are best adapted to spatial variability in soils (Moulia 2013).

1.3 Functions and soil regions of different roots classes

The root system consists of different types of roots. In monocotyledonous plants, first two distinct root classes emerge during seed germination from the embryo (Yamauchi et al. 1996), the primary root and a pair of seminal roots (Nakamoto & Oyanagi 1994; Pflugfelder et al. 2021). This embryonic root system is crucial for the establishment of the plant (Yamauchi et al. 1996). The different root classes grow in different directions and take over different functions. Thereby, the primary root grows steep to penetrate deep soil strata fast in order to reach deep water pools and anchor the plant (Dardanelli et al. 2004; Bellini et al. 2014). In contrast, the seminal roots grow shallow (Nakamoto & Oyanagi 1994) to build a network in the topsoil in order to acquire immobile resources such as phosphorus, potassium and ammonium (Yamauchi et al. 1996; Lynch 2013).

As described before, the soil shows heterogeneities even on a plant root scale (Hodge et al. 2009). Therefore, it is possible that the different roots of a root system hit on different local conditions in the soil. However, as the cells of the different roots are connected by their cell walls, they can send hormonal signals over multiple cells (Robinson et al. 2013). They therefore react and are dependent on the soil conditions of the other roots in the root system (Crossett et al. 1975).

By down-regulating growth under sub-optimal conditions and promoting growth under favourable conditions (Wightman et al. 1980), plants thereby invest in parts, where the gains for the plants are more likely to equalize the investment (Maina et al. 2002). In a root system, where the different roots are competing for nutrients and

assimilates from the endosperm and other parts of the plant, unfavourable conditions of one root might stimulate the growth of another competing root, which might lead to a change in root morphology and growth direction (Crossett et al. 1975; Nakamoto & Oyanagi 1994).

This could be shown in studies on nutrients, where on split-nutrient rhizoslides, roots decreased their growth when their neighbouring roots were exposed to nitrogen pools to promote the growth under the more favourable conditions (in t'Zandt et al. 2015). In experiments on wheat, it could also be observed how a change in growth direction and root diameter occurs to compensate for the loss of other roots (Nakamoto & Oyanagi 1994). Here, an excision of the primary root, led to a steeper growth of the seminal root, while no change occurred for the primary when the seminal root was excised (Nakamoto & Oyanagi 1994). As the distribution among the different types of roots is limited by vascular connection (Bengough et al. 2006; Melnyk 2017) only nearby pairs were influenced.

1.4 Challenges in root research and potential of image-assisted growth quantification

As described in the previous chapter, root responses to different soil conditions are of great interest for science. Especially the underlying processes on a tissue level might give important insights on how roots react to their surrounding conditions. Hence, there is need for more visualized data of the root system (Koevoets et al. 2016) and for more quantitative mechanical data from cell flows and tissues (Forterre 2013).

However, doing research on roots faces challenges (Ingram & Leers 2001). As their natural habitat is soil, which is opaque, the observation of roots in situ and their responses to soil heterogeneities remains difficult. By excavating the root to investigate it quantitatively, the risk of damaging the root increases significantly and root biomass can get lost. Moreover, a direct effect of changing conditions cannot be measured in real-time as the removal of the root causes a delay for the observation (Waisel et al. 2002).

To overcome the challenges of root research, hydroponics represents a well-controlled system, where no root manipulation is needed and therefore no damage of the root occurs (Bizet et al. 2015; Nguyen et al. 2016). It has already widely been used in scientific research to investigate nutrient requirement and toxicity to plant roots (Kopittke et al. 2010; Conn et al. 2013). Looking at the response to a specific condition of several roots at the same time, it offers a controlled environment with real-time results (Nguyen et al. 2016). In combination with near infra-red imaging systems, which can capture temporal variations of in-vivo measurements (Bizet et al. 2016), this can be used to investigate root growth. To elucidate its underlying

processes, kinematics offers a good method (Moulia 2013). Kinematics has already widely been used in investigating the influence of environmental factors on growth patterns of plant roots (Sharp et al. 1988; Yamaguchi et al. 2010) and to investigate the underlying processes of root growth (Beemster & Baskin 1998). In earlier times, this was applied on roots by growing them on a medium plate and observing them under a microscope. A camera then took series of overlapping images (Beemster & Baskin 1998).

Nowadays, the Particle Image Velocimetry (PIV) technique allows to measure a velocity field for a sequence of images and a quantitative identification of spatial-temporal structures (Py et al. 2005). Thereby, particles of moving tissues get illuminated and captured with a camera. The individual particles in the images are then segmented (Adrian & Westerweel 2011) and divided into sub windows. By using a cross-correlation function, the displacement of the different particles between the images, hence the movement of the tissue particles, can be determined (Bastien et al. 2016). Knowing the time between the different images, the velocity can be calculated (Py et al. 2005). PIV has for instance been applied to do kinematic analysis of root growth (Bizet et al. 2015) and to study cell division and root elongation rate of *Populus* (Youssef et al. 2018). Therefore, this method provides insights in complex organ movements (Bastien et al. 2016).

1.5 Aim of the study

As elaborated before, research has widely been studied how roots react on different soil conditions (Clark et al. 2003; Jin et al. 2013; Bizet et al. 2016). Moreover, in previous studies, it could be shown that roots also react on the root growth conditions of other roots in their root systems (Nakamoto & Oyanagi 1994; in t'Zandt et al. 2015). Nevertheless, it remains unclear to what extend the restriction of one root influences the growth of the other roots.

Hence, the aim of this study is to contribute to existing research by understanding how roots adjust their growth behavior, such as their growth rate and direction in response to a growth restriction due to local mechanical stress in the root system. Thereby following research questions were invesitgated:

1. How does root growth direction of an unimpeded root react if another root is impeded?
2. How does root growth rate of an unimpeded root react if another root is impeded?
3. What drives root growth rate in such a situation? Cell elongation rate or length of the growth zone?)

In order to answer the research questions, in-vivo time-lapse imaging was carried out to seeds of wheat (*Triticum aestivum* L.*).* Pre-germinated seeds were grown in a nutrient solution. Obstacles of different orientations for different roots simulated mechanical stress in form of microscope slides pasted with sand. For a high-resolution root growth quantification, a time-lapse imaging system was developed to quantify root growth. The image processing program ImageJ and the Matlab application KymoRod (Bastien et al. 2016) allowed the quantification of the underlying root growth processes.

2. Materials and Methods

2.1 Experimental set-up

During the experiment, wheat seeds were grown in a customized growth container with a volume of 3.5 l containing a half-strength Hoagland nutrient solution (Sigma Aldrich Solutions, Merck KGaA, Darmstadt, Germany).
Consisting of 15 mm thick Plexiglass, the growth container enabled a good observation of the root growth. The dimensions of the glass container were 40 x 15 x 5 cm. A metal frame constructed by metal bars stabilized the growth container (Fig 2A).

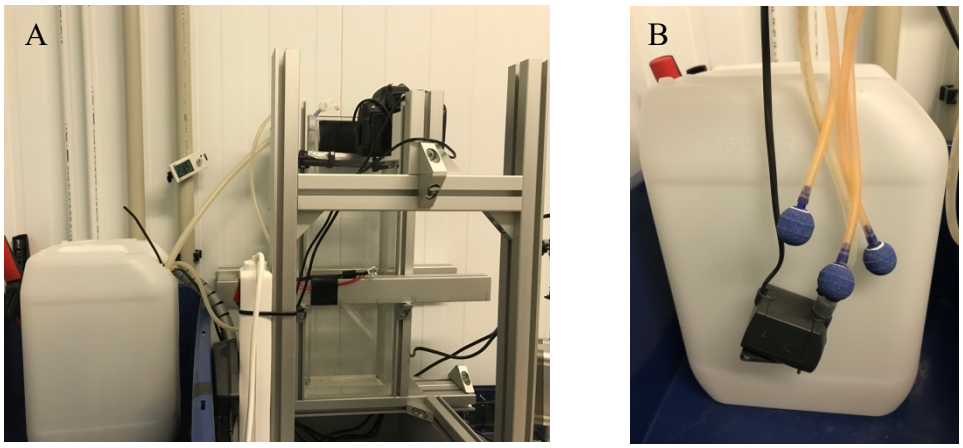

Figure 2: Experimental set up with the growth container containing the nutrient solution (A) and the plasticcontainer containing the pumps, which pumped the solution over the tubes into the growth container and brought oxygen into the system (B).

The growth container was filled with a nutrient solution of pH 5.8. Therefore, 100 mL of 0.25 M NaOH were prepared to adjust the pH of the final solution. To prepare the final solution the Hoagland's No. 2 Basal Salt Mixture was diluted in a fume hood to reach a 50 % Hoagland solution. Each weak, 10 l nutrient solution were used. It was filled in a 15 l tank. To avoid hypoxia, the nutrient solution was

aerated with three pumps (JBL PROSILENT a100, JBL GmbH & Co. KG, Germany). The aerated final solution was pumped to the growth system by an aquarium pump (NEWA Jet 400 – 600, Newa Tecno Industria SRL., Italy) and was returned through an outlet, so that a circulation between the tank and the growth system was ensured (Fig. 2B). The nutrient solution in the tank and the growth system was exchanged once a week.

2.2 Treatments

The growth system consisted of two Plexiglas sheets, which were held together by four screws. To ensure a good growth for the visualization, one of the Plexiglasses was glued with small pieces of black tape guiding the channels for the different roots (Fig. 3A).

The seed was placed with tweezers into these channels and covered with a filter paper. After screwing the plexiglasses together, the growth system was placed into the nutrient solution in the growth container, where it was hold on top by extended screws. To ensure that the seed was wetted over the whole experimental period, the filter paper in the growth system had to be in contact with the nutrient solution.
To investigate the impact of localized mechanical stress on the root growth, the root was restricted in its growth by obstacles of different orientations and positions, which are illustrated in figure 4. The obstacles were represented by a microscope slide pasted with sand (4.5 x 1.5 cm), which was fixed on a plastic holder (Fig. 3B).

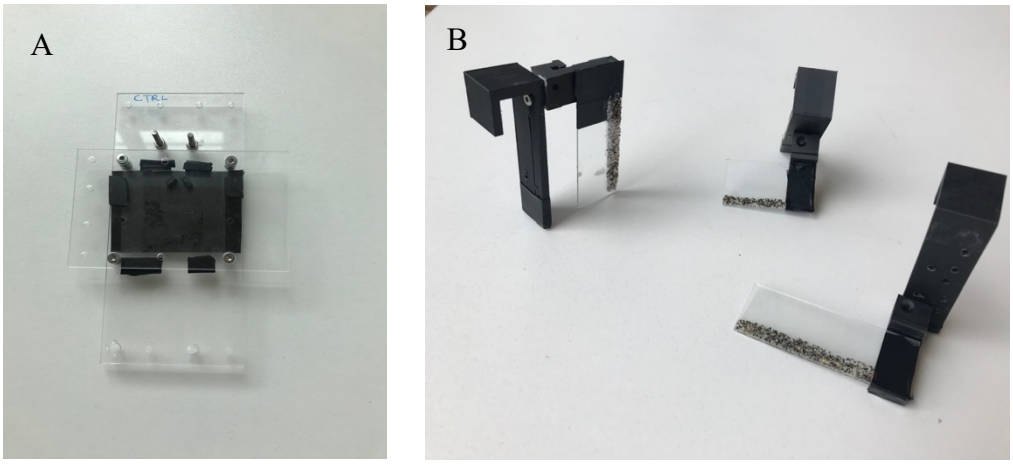

Figure 3: Plate with stacks of rubber band to guide the root growth (A) and the seminal vertical, seminal horizontal and primary horizontal obstacle (from left to right) in form of microslides with pasted sand (B).

In one treatment the primary root was hindered by a horizontal obstacle (PH) (Fig. 4B). The other two treatments were applied to the seminal roots. Here, one obstacle (SH) hindered the seminal root horizontally (SH) (Fig. 4C), while the vertical obstacle restricted the seminal root in their lateral root growth (SV) (Fig. 4D). All the treatments were compared to a control group (Fig. 4A), where no obstacle was used. Each treatment was replicated 4 times. The growth system and the obstacles were hooked into the set-up and fixed with a metal clamp.

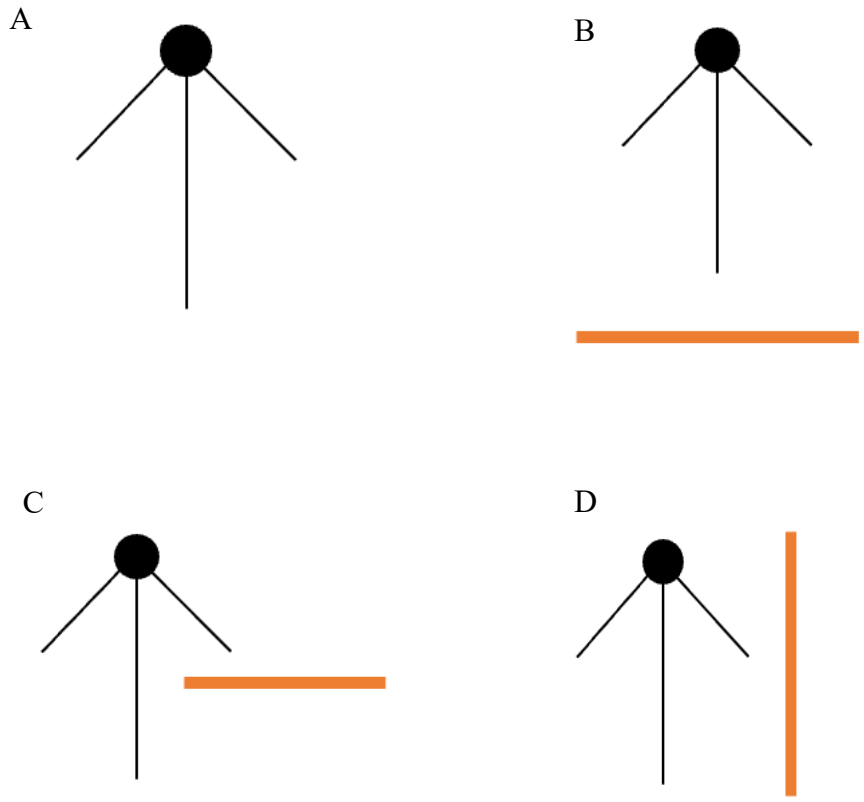

Figure 4: Schematic scheme of the control treatment (A), the primary horizontal treatment (B), the seminal horizontal treatment (C) and the seminal vertical treatment (D).

2.3 Plant material & growth conditions

For the experiment, spring wheat (*Triticum aestivum* L.) seeds of the variety "Happy" were used. To ensure that the seeds grow as equally as possible, seeds of similar weight were selected beforehand. Using an analytical balance (Mettler Toledo, Switzerland), seeds of an average weight of 40 mg with a range of +/- 10 % were chosen for the experiment.

10 seeds were pre-germinated between filter paper (Fig. 5) in a large tray (30 x 15 x 10 cm) filled with the 50 % nutrient solution (Fig. 6). The germination time amounted to 56 – 63 hours and seedlings with similar root length were selected for the experiment (Tab. S2). During this time the box with the filter paper was covered with aluminium foil. The temperature in the climate-controlled growth chamber was constantly 20 °C. After the germination time one seed of a primary root length of 1.9 to 2.8 cm were chosen for the experiment.

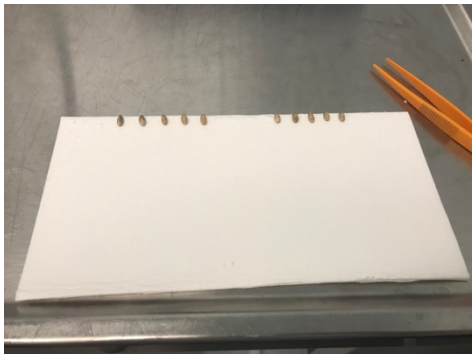

Figure 5: Pre-germination of 10 seeds on filter paper.

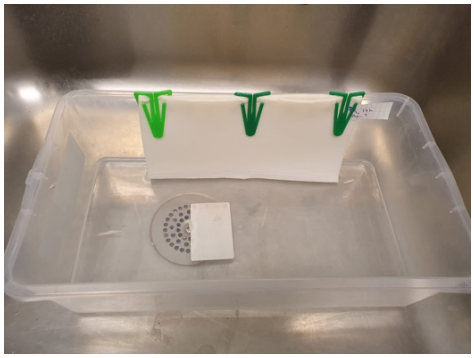

Figure 6: Plastic box with Hoagland solution to pre-germinate 10 seeds.

2.4 Time-lapse imaging

The growth container was fixed in a metal frame constructed by aluminium bars in a temperature regulated room. A time-lapse imaging system was installed 6 cm in front of the experimental set-up. The time-lapse imaging took place in darkness. To visualize the roots, but not influence the root growth, roots were illuminated by 10 infrared lights with a wavelength of 830 nm (Vishay, Malvern, USA) (Fig. 7). The infrared filter of a Canon EOS 750D (Canon, Tokyo, Japan) camera was removed. Having a 24.2 megapixels resolution, the pixel edge length amounted to 8.8 µm. To

obtain optimal image quality, the settings of the camera consisted of an exposure time of 1/20 seconds, aperture value of f/9.0 and ISO of 100.
The roots grew in the system for 24 hours and the camera took pictures every 2 minutes. The pictures were saved as JPG.

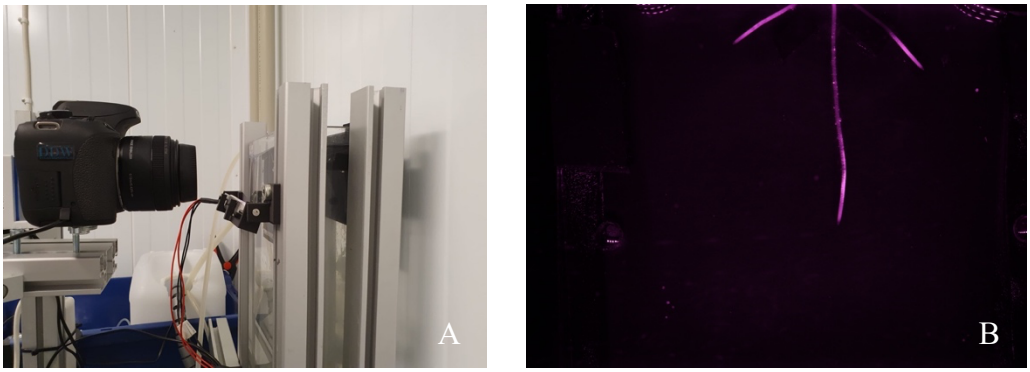

Figure 7: Time-lapse imaging system with a Canon EOS 750D (A) and an image taken by the imaging system under the infra-red lights (B).

2.5 Imaging processing

2.5.1 ImageJ

Images from a time span of 2 hours before and 4 hours after the root reached the obstacle were chosen for the analysis. For the control treatment an average of the images, which represented the mentioned time span of analysis, was calculated. This ensured that pictures of all treatments represented 6 hours around the reach of the obstacle (Tab. S3). The software ImageJ (ImageJ, National Institutes of Health, Bethesda, USA) was used to pre-process the images for further analysis. As each root was analysed separately, the single roots were isolated in ImageJ so that image series of every individual root originated. Moreover, noises (water bubbles, air bubbles or clue of the rubber band stacks) in the images were cut out with the software. To isolate each root, a macro, which automates a series of ImageJ commands, was recorded (ImageJ 2022). The last image of one time-lapse series served to mark the to-analysing roots by using the polygon selection function. ImageJ was then able to recognize the size markers and their x- and y- coordinates in the images and therefore copied the marked root to a new image, which was saved as a .TIFF file. Using the batch processing function enabled the application of the macro commands to the whole image series.

2.5.2 KymoRod

The Matlab (The MathWorks Inc., Natick, Massachusetts, USA) application KymoRod v0.11.0 (Bastien et al. 2016) was used to calculate elongation and curvature profiles. The software first imported the pre-processed image stack of the time of 2 hours before and 4 hours after reaching the obstacle (Fig. 8A and 8B). For every image series, segmentation thresholds were set manually (Tab. S1) (Fig. 8C). A skeleton of the contour was computed automatically (Fig. 8D) by using the Voronoi diagram of the contour (Clément et al. 2012). The midline of the contour was recognized and extracted as the longest branch within the skeleton. Along this midline, the curvilinear abscissa got calculated. Using a Rod-PIV approach (Bastien et al. 2016), also enabled the calculation of the elongation rate along the midline (Fig. 8E). In the Rod-PIV approach, the sub-windows are located on the midline of the organ. The moving sub-windows are then correlated to the sub-windows of the previous image, which was taken at an earlier time to calculate the velocity (Bastien et al. 2016). A complete overview of the settings used for image analysis in KymoRod is provided in appendix (Tab. S4).

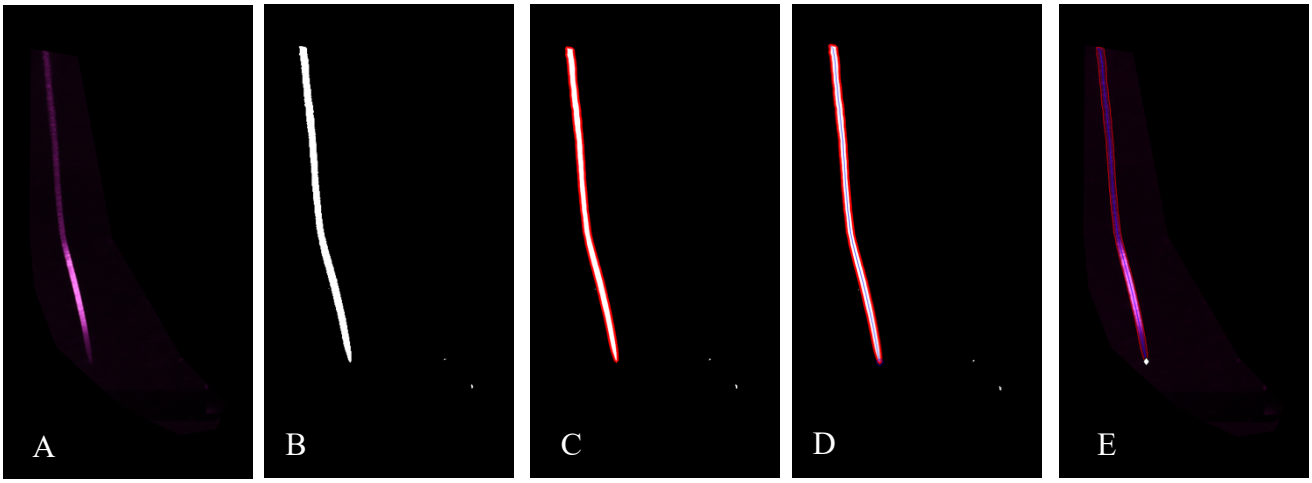

Figure 8: Pictures of a primary root of 2h before reaching the obstacle (A), after uploading in ImageJ (B), after contouring the skeleton (C), after extracting the midline of the skeleton (D), after displacement (E).

2.5.3 Data processing

R version 4.1.0 extracted growth rate, growth zone, curvature, elemental elongation rate and elongation zone profiles from the KymoRod files using the packages "R.matlab" (Bengtsson, 2018) and "RColorBrewer" (Neuwirth, 2014). The root

growth rate, the elemental elongation rate and the length of the growth zone were all calculated based on the velocity profile along the midline of the skeleton. The plateau of the velocity profile, respectively the maximum velocity represents the growth rate [mm h^{-1}]. The derivate of the velocity profile corresponds to the elemental elongation rate [h^{-1}] (Fig 9). The point, where the maximum elemental elongation rate is reached is used to describe the cell elongation rate. Thereby, xEERmax describes the position, along the central axis of the root at which the maximum elemental elongation rate occurs. The end of the growth zone was defined as the zone between the root tip and the point, where the elemental elongation rate decreased below 2 %, accordingly, the point, where the maximal velocity is reached (Fig 9).

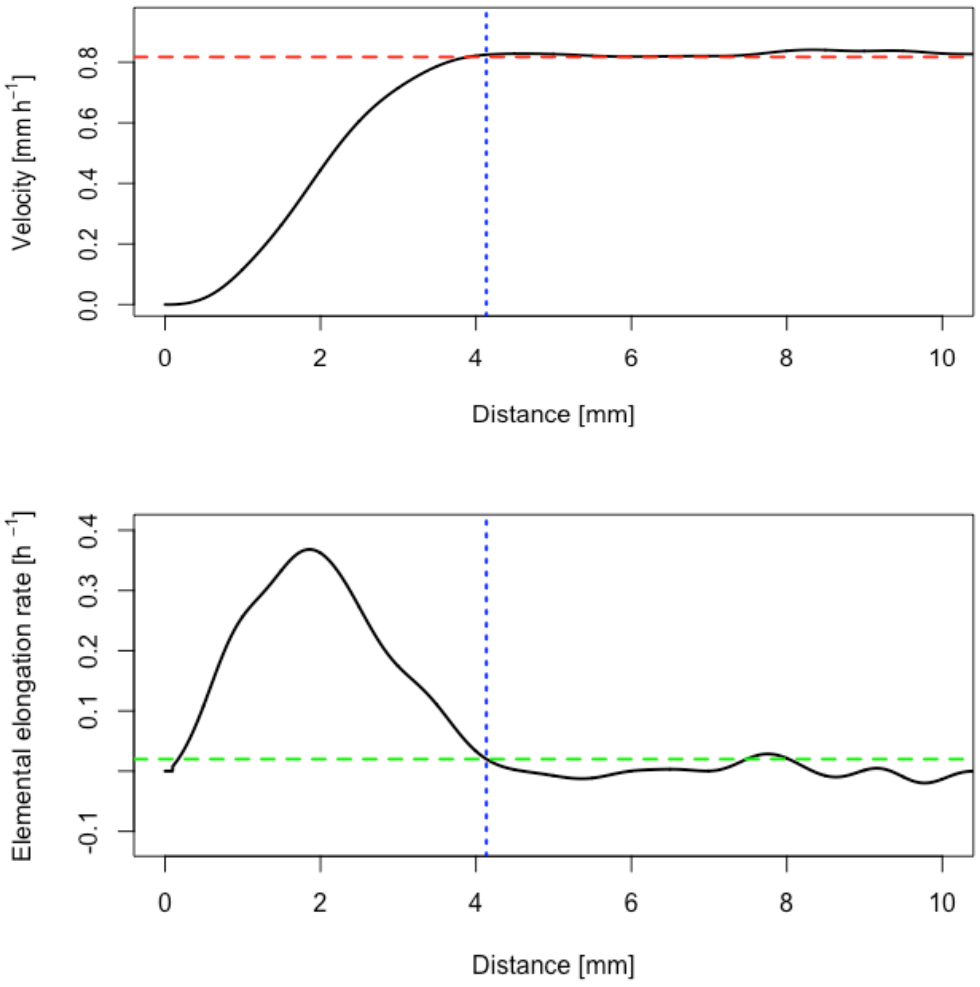

Figure 9: Illustration of the determination of the elemental elongation rate, the growth rate and the growth zone.

The curvature was calculated from the curvature profile from KymoRod as the average curvature in the growth zone. Negative values thereby indicate a shallow, plagiotropic growth, while positive values represent a steep, gravitropic growth. To account for the different initial root directions of the right and left seminal root, the curvature values of the right seminal roots were multiplied with -1. Raw data was filtered by using an upper filter of 4 * the average of the xEERmax and a lower filter limit of ¼ * average of the xEERmax. Moreover, a second filter sorted out all values of the growth rate, which were lower than 0 mm h^{-1} and higher than 3 mm h^{-1}. Only runs with an error rate below 10% were taken into the statistic (Tab. S1).

2.6 Statistical analysis

Statistical analysis was carried out in R version 4.1.0 (R Core Team 2020). For this, hourly mean values calculated by R were used for all the parameters.
For treatments, in which the growth rate was calculated for both seminal roots (control and primary horizontally), a mean value of the right and left root was taken. All values were represented in absolute values. For the growth rate, the elemental elongation rate and the length of the growth zone, relative values were additionally calculated, which represent the ratio of the value after the reach of the obstacle to the average of the values before the reach of the obstacle. For the curvature, the differences between the values after the reach of the obstacle and the average of the values before the reach of the obstacle were calculated.
As repeated measurements were done, a linear mixed effective model was used to evaluate the effect of local soil mechanical stress and time on the root growth rate.

Using the package "nlme" for the model (Pinheiro et al. 2017), the following model was separately applied to the primary root and the seminal root in order to evaluate the effects of treatment, time, and their interaction on the different roots:

$$Y_{ij} = a_i + \beta + a\beta_i + y_j + r_{ij} \, (Eq. 1)$$

where Y denotes the root growth rates of the i^{th} treatment (i = obstacle, primary root horizontal, seminal root horizontal, seminal root vertical, control), and the j^{th} sample (j= 1, 2, 3, …, 16). The effects of the treatment (α), the time (β), and their interaction (αβ) were set as fixed effects. The sample effect (γ) was set as a random effect to account for repeated measurements. The residual error is described by r. An analysis of co-variance was used to test the significance of the fixed effects. A least significant difference (LSD) test compared the means of the different treatments within the same hours before and after reaching the obstacle using the 'agricolae' package (de Mendiburu, 2017).

3. Results

3.1.1 Root growth quantification

Based on the graphs produced by R Studio, the root curvature and growth rate could be illustrated. Figure 10 shows how the orientation of the root was recognised by the software and displayed as the curvature in growth zone in a graph. If the root changed its direction to a shallower root growth, the curvature showed negative values. If it bent to a rather steep growth, the curvature reached positive values.

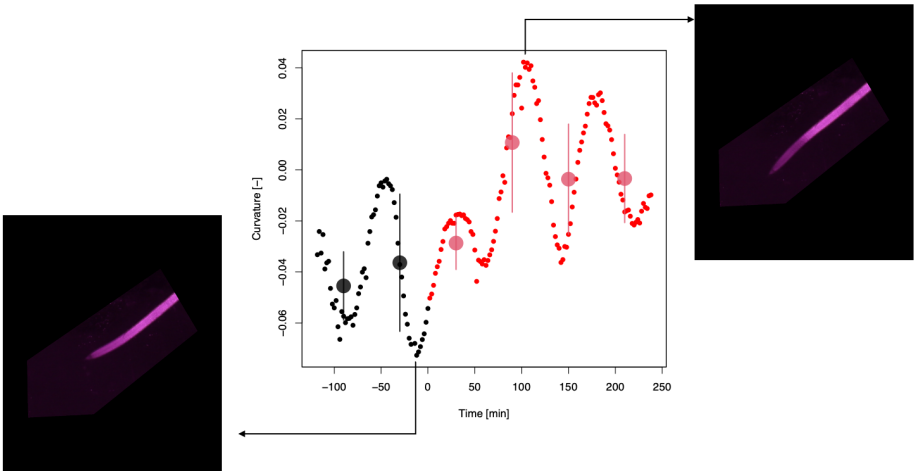

Figure 10: Typical example of the temporal development of the curvature in the root growth zone captured by the time-lapse imaging system, and illustrated by R. Bending to a shallow growth, results in a negative curvature, bending to a steeper growth results in positive curvature values.

A comparison between the change in the growth rate of the root captured by the time-lapse imaging system and the growth rate illustration in the graph produced with R, can be seen in figure 11. The rather low root growth rate during the time before reaching the obstacle (minute -100 to -50) describes the only slightly visible change in length of the root between the first two pictures. On the other hand, the higher growth rate during the last 50 minutes can be observed in the difference between the last two pictures.

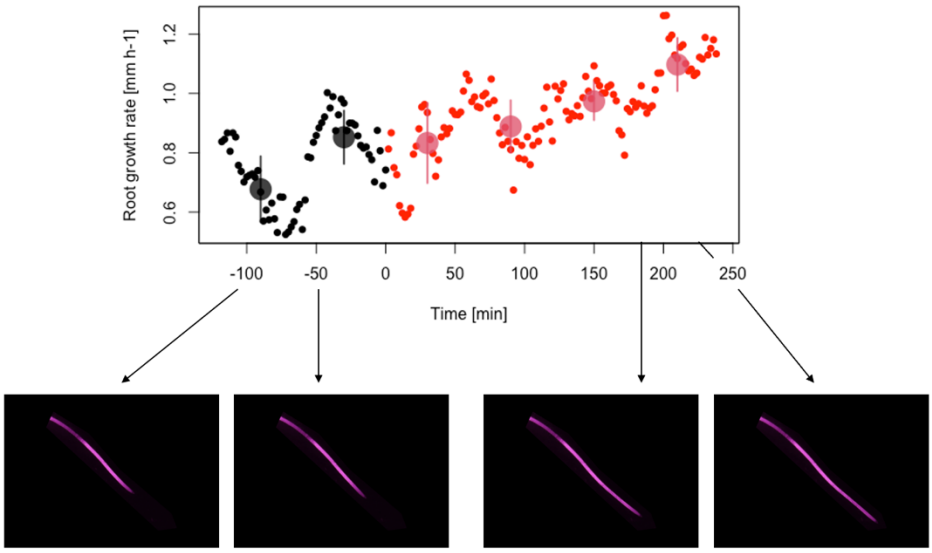

Figure 11: Typical example of the temporal development of the growth rate [mm h^{-1}] captured by the time-lapse imaging system, and illustrated by R.

Similar to the growth rate, the elemental elongation rate (Fig 12.) could be displayed in a graph by R. When the cell elongation was low (minute -50 to -25), this was represented by a low maximal elemental elongation rate in the graph.
In contrast, the root elongated faster during the last 25 minutes. This faster elongation is also shown by higher values of the maximal elemental elongation rate in the graph (Fig. 12).

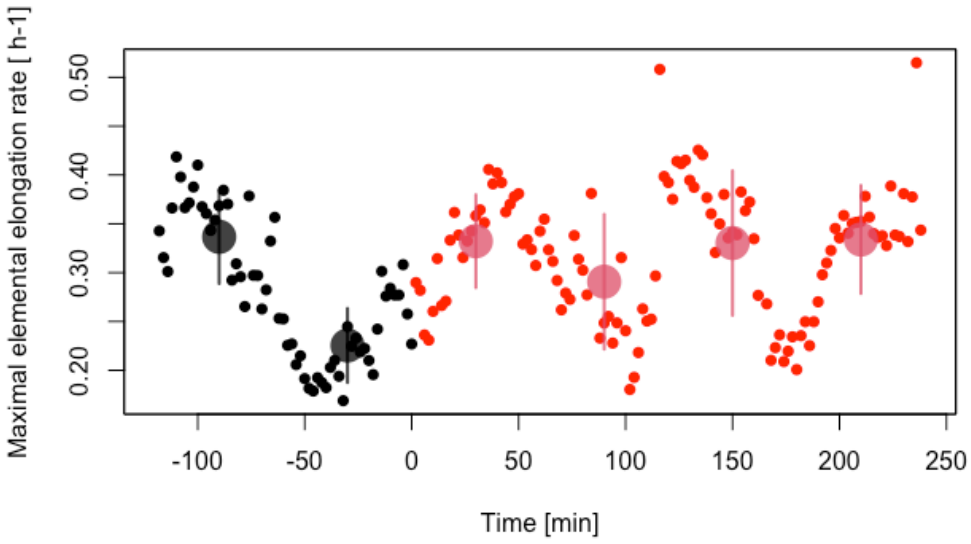

Figure 12: Typical example of the temporal development of the elemental elongation rate [h^{-1}] captured by the time-lapse imaging system, and illustrated by R.

Figure 13 shows the growth length captured by the time-lapse imaging system and the graph illustrated by R. Two hours before the obstacle was reached, the root showed a low growth zone length of 4 to 4.5 mm. Until the end of the analysis, the length of the growth zone increased up to around 6 mm, which was then also represented by a longer length of growth zone in the graph (Fig. 13).

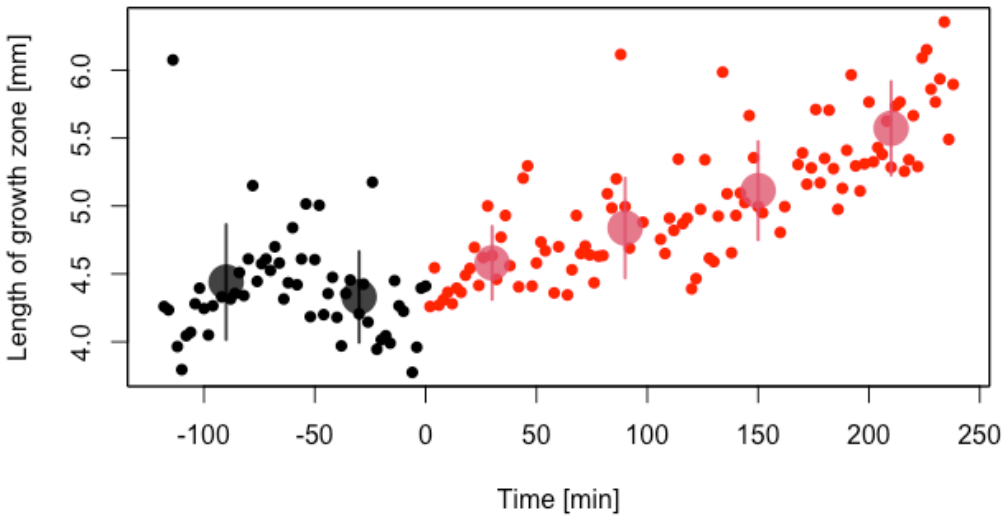

Figure 13: Typical example of the temporal development of the length of the growth zone [mm] captured by the time-lapse imaging system, and illustrated by R.

3.2 Effects of obstacles on root growth direction and root growth rate

3.2.1 Responses of root growth direction to mechanical obstacles

For the curvature, values of differences were calculated which represented the difference in curvature in the growth zone between the values after reaching the obstacle and the average of the curvature values during the time before reaching the obstacle.

Table 1: Effect of treatment, time and their interaction on the difference in curvature of the growth zone [-] for the primary root (PR) and the seminal roots (SR) (Eq.1, n=4).

	PR	**SR**
Effects	**p value**	**p value**
Treatment	0.741	0.693
Time [min]	0.696	0.402
Treatment:time	0.53	0.22

For the primary roots, no treatment changed its growth direction after the obstacle was applied (Fig. 14A). The primary roots whose second seminal roots were impeded (SH and SV), slightly grew shallower over the whole time of analysis, but differences only amounted from 0.048 to – 0.017. Roots which were not exposed to obstacles, changed from a shallower to a steeper and back to a shallower growth direction (Fig. 14A). However, neither the linear mixed model, nor the post-hoc analysis showed a significant effect of the treatments (Tab. 1).

In contrast to the primary roots, the growth direction of the seminal roots changed in response to the obstacle. While during the first hour of analysis, no change could be observed, the growth direction started to differ significantly between the treatments during the second hour (Fig. 14B). While the control did not change its growth direction, the seminal roots, whose neighbouring roots got impeded vertically (SV), changed to a steeper growth. In contrast, both other treatments (PH and SH) showed a shallower growth than during the time when no stress was applied. This started to equal out during the third hour after the reach of the obstacle. Nevertheless, the seminal vertical treatment (SV) still showed a steeper growth direction than the other treatments.

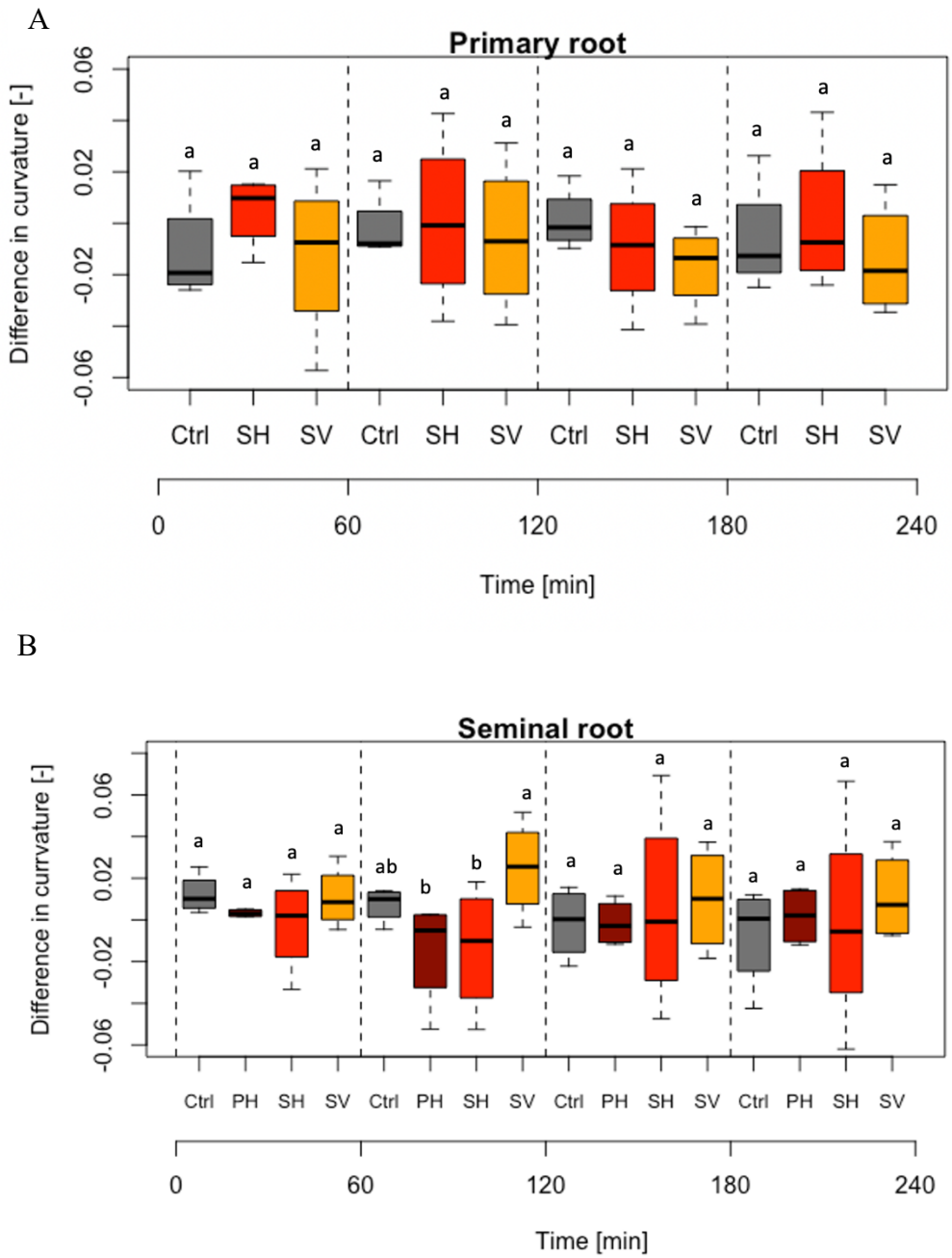

Figure 14:Difference in curvature [-] for control, primary horizontal (PH), seminal vertical (SV) and seminal horizontal (SH) treatment on the primary (A) and seminal roots (B) during the 4 hours after reaching the obstacle. Different letters denote significant differences within one time-point using least significant difference test at p = 0.05 (n=4).

3.2.2 Responses of root growth rate to mechanical obstacles

The absolute values only showed a significant effect in time for both root classes (Tab. 2). However, the absolute values of the different treatments varied already significantly in their growth rate before the obstacle was reached, especially for the seminal roots (Fig 15B). Therefore, relative values, which represented the values after reaching the obstacle in relation to the average of the ones before reaching the obstacle, were calculated. Relative values made the comparison between the treatments more reasonable (Fig. 15 C and D).

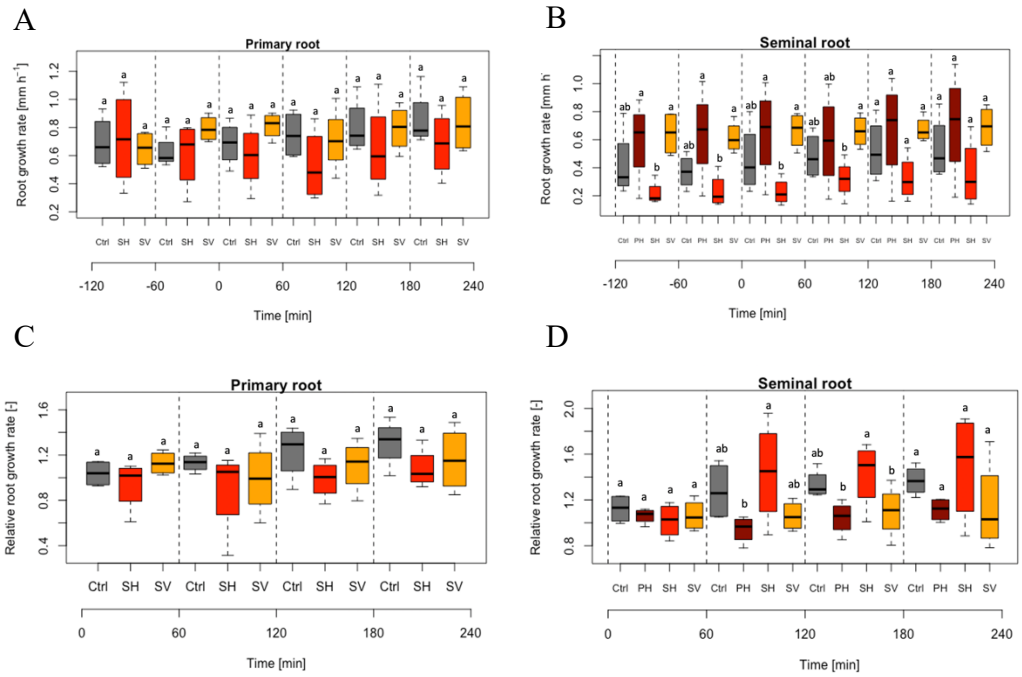

Figure 15: Absolute values (A and B) and relative values (C and D) of the growth rate [mm h^{-1}] for control, primary horizontal (PH), seminal vertical (SV) and seminal horizontal (SH) treatment on the primary (A and C) and seminal roots (B and D) two hours before and four hours after reaching the obstacle. Different letters denote significant differences within one time-point using least significant difference test at p = 0.05 (n=4).

Looking at the relative values, a significant difference could only be seen in time for both the primary and the seminal root (Tab. 2).

For the primary roots, the treatments had no significant effect over the whole time of analysis (Fig. 15C). Despite this, different trends of the different treatments could be observed. Roots which were not impeded increased their relative growth rate by 27 % during the 4 h of analysis. In contrast, the primary roots whose seminal roots were impeded (SV and SH) did not increase their growth rate in response to the obstacle so that they showed a 15 % to 23 % lower relative growth rate than the control at the end of the analysis (Fig. 15C).

Table 2: Effect of treatment, time and their interaction on the absolute (Abs) and relative (Rel) root growth rate for the primary roots (PR) and the seminal roots (SR) (Eq.1, n=4).

	PR		SR	
Effects	**Abs**	**Rel**	**Abs**	**Rel**
Treatment	0.51	0.232	0.094	0.151
Time-min	0.044	0.028	< 0.001	0.001
Treatment:time	0.197	0.487	0.252	0.122

The seminal roots showed no reaction to the obstacle during the first hour (Fig. 15D). During the second hour, the roots which grew under optimal conditions and the ones whose second seminal root were impeded horizontally (SH) increased their relative growth rates, while the other treatments (PH and SV) did not response to the obstacle with an increase in growth rate. Thereby, the seminal horizontal (SH) treatment showed with 1.439 a 17% higher relative growth rate than the control treatment. During the last two hours of analysis, this difference slightly equaled out, so that no significant difference between the treatments could be observed during the last hour. However, the seminal roots of the seminal vertical (SV) treatment still showed an 12% to 37% higher relative growth rate than the other treatments (Fig. 15D).

3.2.3 Responses of the maximal elemental elongation rate to mechanical obstacles

Only the interaction of treatment and time showed a significant effect on the absolute values of the maximum elemental elongation rate for the seminal roots ($p = 0.019$) (Tab. 3). As already seen for the growth rate, significant effect for the treatments could already be observed before the stress was applied (Fig. 16B), which is why relative values were calculated, which made the analysis more meaningful.

For the relative values, treatment, time and the interaction of treatment and time did not show a significant effect for both root classes (Tab.3). Nevertheless, trends could be observed. The primary roots showed no response to the obstacle during the first hour (Fig. 16C). During the second hour, the primary roots, whose seminal roots were impeded vertically (SV) started to slightly decrease its relative elemental elongation rate, while the control treatment increased it. In contrast to the response of the relative growth rate, also the relative elemental elongation rate of the seminal horizontal (SH) treatment increased, so that it was 43% higher than the relative

elemental elongation rate of the seminal vertical (SV) treatment during the third hour after the reach of the obstacle. During the last hour this difference equalled out (Fig. 16C).

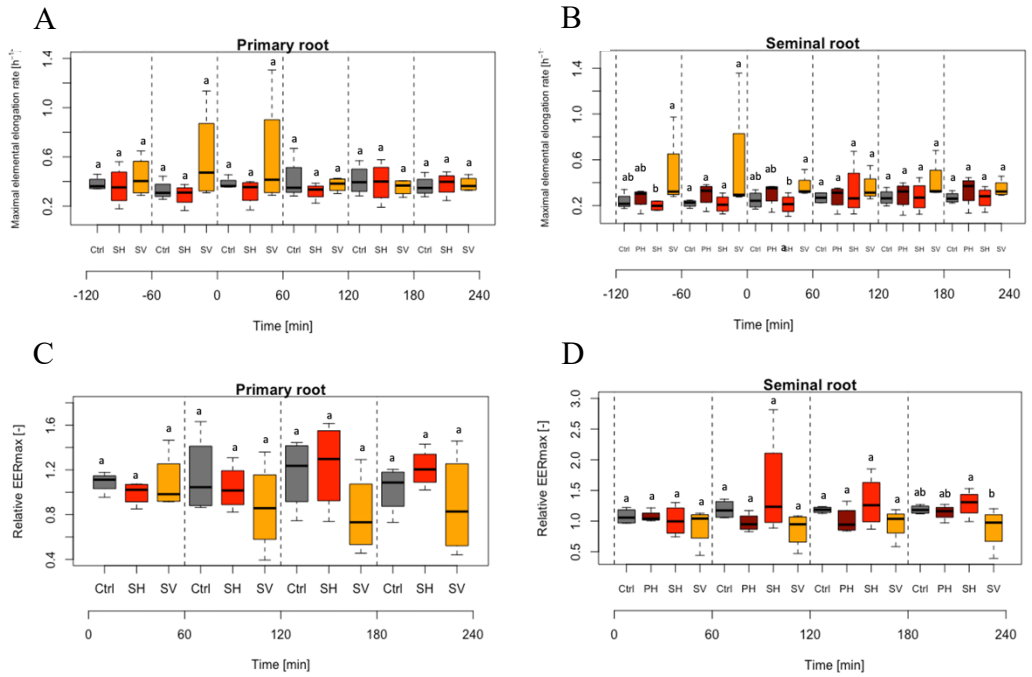

Figure 16: Absolute values (A and B) and relative values (C and D) of the maximal elemental elongation rate [h^{-1}] for control, primary horizontal (PH), seminal vertical (SV) and seminal horizontal (SH) treatment on the primary (A and C) and seminal roots (B and D) two hours before and four hours after reaching the obstacle. Different letters denote significant differences within one time-point using least significant difference test at p = 0.05 (n=4).

Table 3 Effect of treatment, time and their interaction on the absolute (Abs) and relative (Rel) maximal elemental elongation rate for the primary roots (PR) and seminal roots (SR) (Eq.1, n=4).

	PR		SR	
Effects	**Abs**	**Rel**	**Abs**	**Rel**
Treatment	0.458	0.375	0.305	0.218
Time-min	0.492	0.965	0.814	0.133
Treatment:time	0.089	0.104	0.019	0.744

The treatments of the seminal roots showed trends, which were more in line with the response of the growth rate. During the first hour, no reaction could be observed (Fig. 16D). As already seen for the relative growth rate, the roots which were not impeded and the ones whose second seminal roots were impeded horizontally (SH)

started to increase their relative elemental elongation rate during the second hour. Thereby, the increase of the SH treatment was 17% higher than the one of the control treatment. In contrast, the primary horizontal (PH) and seminal vertical (SV) treatment started to decrease their relative elemental elongation rate over the whole period of analysis, so that the seminal vertical (SV) treatment showed a 40% lower relative elemental elongation rate than the seminal horizontal (SH) treatment (Fig. 16D).

3.2.4 Responses of the length of growth zone to mechanical obstacles

Looking at the absolute values for the length of the growth zone, one can see, that the treatments already had a significant impact before the obstacle was reached (Fig. 17 A and B). As already done for the growth rate and the elemental elongation rate, relative values were therefore calculated in order to compare the treatments.

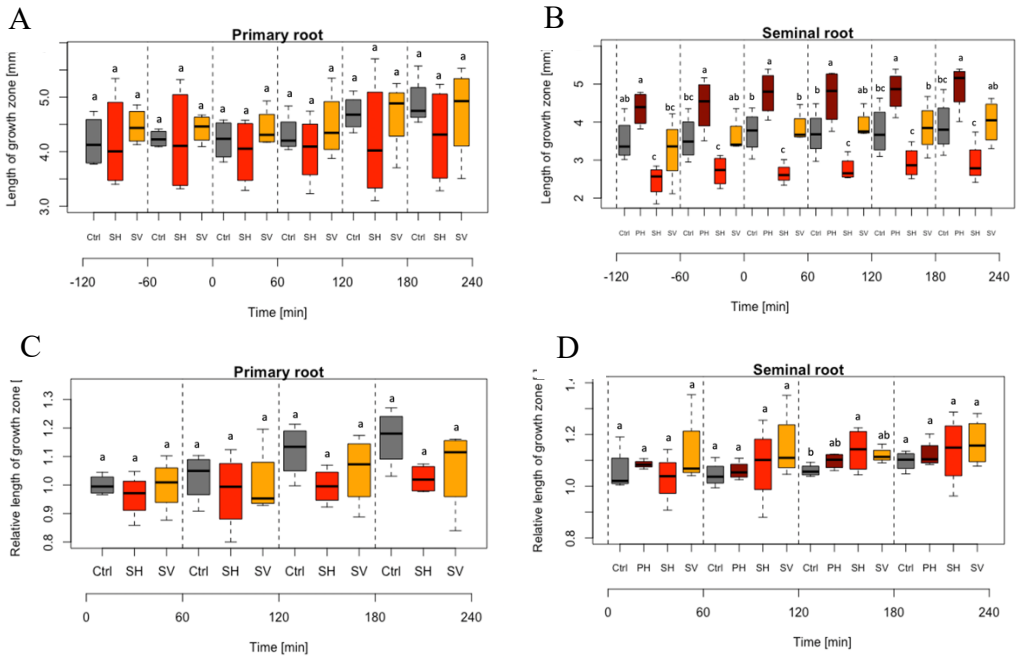

Figure 17: Absolute (A and B) and relative (C and D) length of the growth zone for control, primary horizontal (PH), seminal vertical (SV) and seminal horizontal (SH) treatment on the primary (A and C) and seminal roots (B and D) during the 4 hours after reaching the obstacle. Different letters denote significant differences within one time-point using least significant difference test at p = 0.05 (n=4).

Thereby, the responses differed significantly in time for the primary roots (p = 0.0003) and the seminal roots (p = 0.006) (Tab. 4). However, neither the treatment nor the interaction of treatment and time showed a significant effect.

Table 4: Effect of treatment, time and their interaction on the absolute (Abs) and relative (Rel) root growth rate [-] for the primary roots (PR) and the seminal roots (SR) (Eq.1, n=4).

	PR		SR	
Effects	**Abs**	**Rel**	**Abs**	**Rel**
Treatment	0.645	0.339	0.003	0.517
Time-min	0.001	0.0003	<0.001	0.006
Treatment:time	0.048	0.111	0.365	0.367

It could be seen that the relative growth zone length of the primary root followed the same trend as the relative growth rate of the primary roots. While the relative length of the growth zone of the control treatment increased over the whole 4 hours after the obstacle was reached (Fig. 17C), the primary roots, whose seminal roots were restricted vertically (SV) only showed an increase in growth zone length during the last two hours after a decrease during the second hour of analysis. The primary roots of the seminal horizontal (SH) treatment only increased slightly during the 4 hours of analysis but decreased by up to 4% compared to the time when no stress was applied (Fig. 17C).

Again here, for the seminal roots a significant effect of time could be observed (p = 0.006) (Tab. 4). All treatments increased their relative length of growth zone over the whole time after the obstacle was reached. Thereby, significant differences between the treatments could also be observed (Fig. 17D). In contrast to the primary roots, the relative growth zone length of the seminal roots did not show the same pattern as the relative growth rate. The growth zone length of the roots whose second seminal roots were restricted horizontally (SH) increased strongly during the first three hours by 11% so that their growth zone length was significantly higher than the one of the other treatments (Fig. 17D). In contrast to the relative growth rate, also the relative length of growth zone of the primary horizontal (PH) and seminal vertical (SV) treatment increased. Thereby, the primary horizontal (PH) treatment increased its relative growth zone length only slightly faster than the control treatment, while the roots of the seminal vertical treatment (SV) increased it in a way that it was even higher than the one of the seminal horizontal (SH) treatment at the end of the analysis (Fig. 17D).

3.3 Methodological challenges

Using a method for the first time brought some challenges which affected the quality of the results.
First, the analysis of some runs was not possible at all. As some seedlings were big at the time of transplanting, they grew out of the picture during the 4 hours after the root reached the obstacle (Fig. 18). The problem occurred mainly for the seminal horizontal treatment, as here, the size of the obstacle let the test plate appear far left in the picture. To overcome this challenge, smaller roots were taken, and the rubber band stacks were adjusted in order to ensure images of the whole root during the 4 hours after reaching the obstacle.

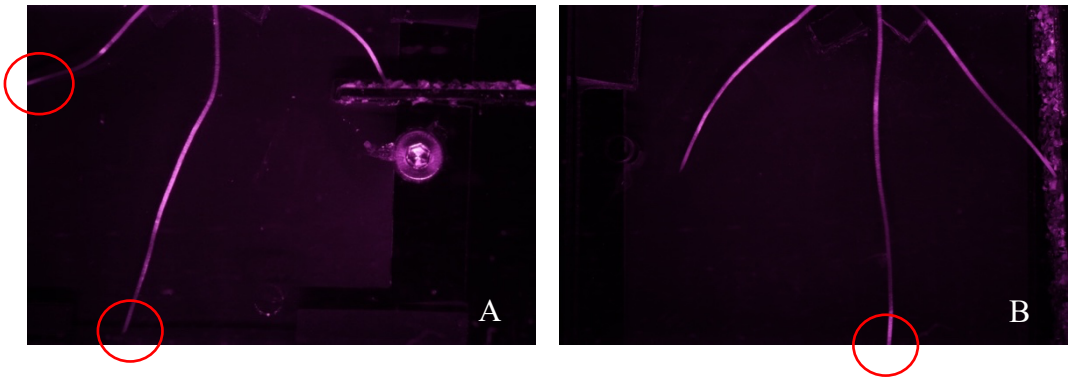

Figure 18: Left seminal root and primary root of Run 10 (A) and primary root of Run 12 (B) growing out of the picture 4h after reaching the obstacle.

Another challenge was, that the roots did not show a sufficient growth. Either the left or right seminal root grew too slow so that the obstacle was not reached during the 24 hours of time-lapse imaging (Fig.19). Therefore, these time-lapse series were not analyzed at all, or the analysis was not valid as negative growth rates occurred.

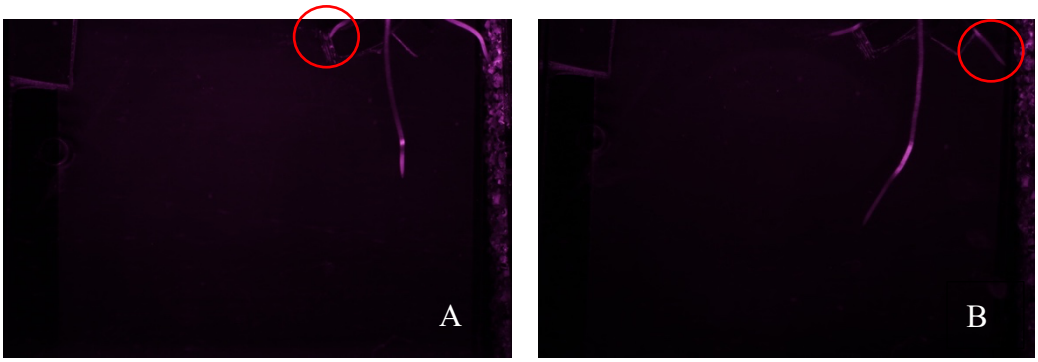

Figure 19: Limited root growth of the left seminal root of Run 23 (A) and the right seminal root of Run 37(B).

Further challenges occurred during the analysis of the images. Some roots grew as close to the rubber band stacks, that the first part of the root disappeared partly in the shadow of the channels (Fig. 20A). This prevented KymoRod from finding enough points for the contour of the root. For other treatments the channel posed a problem in the sense that the clue of the rubber strips became visible on the pictures through the infrared lights (Fig. 20B). This in contrast led to the fact that these points were also recognized by KymoRod. In those cases, where the root grew close to the channels, these points were then merged with the points of the root, so that a distorted contour of the root got extracted by KymoRod, which influenced the error rate of the analysis.

The analysis with KymoRod could also be negatively hampered by small residues on the plate (Fig. 20C) or little air or water bubbles, which occurred close to the root. Also, for these runs, the unwanted points got recognized by the software and were included into the root contour (Fig. 21). Here, the settings of the infra-red lights played a crucial role. If the pictures were too overexposed, more noise was visible, which distracted the quality of the pictures. Additionally, the light caused problems for several runs, since the roots grew into a darker spot, where it became hard to detect the individual particles of the root tissue (Fig. 20D). This mostly occurred for the primary root, which is why several runs had to be repeated due to a failed analysis of the primary root.

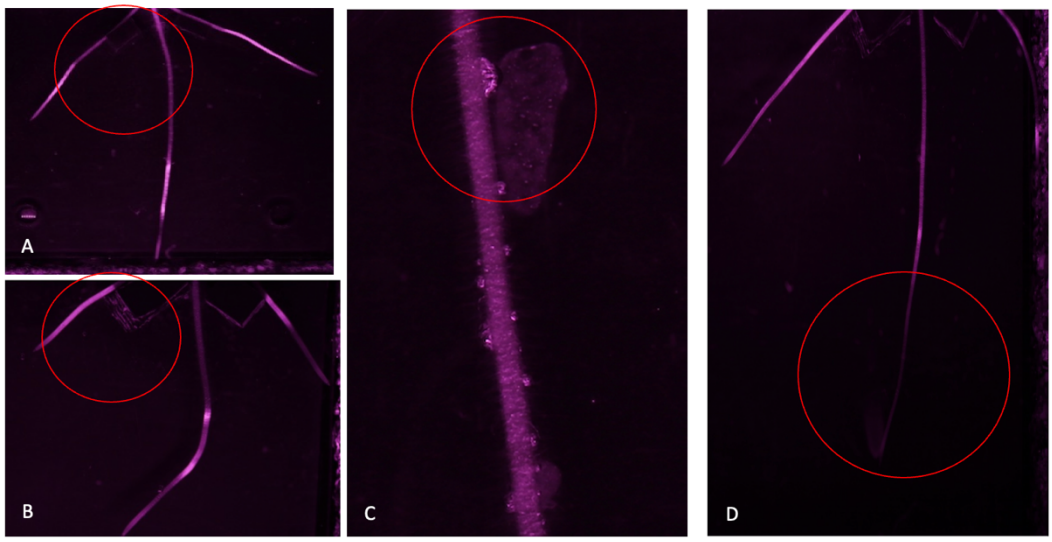

Figure 20: Challenges occurring during the image analysis: Part of the root grew in the shadow of the channel (A), the clue of the channels is visible in the images (B), noises (air bubbles, water bubbles) occur close to the root (C), primary root grows into a dark hole (D).

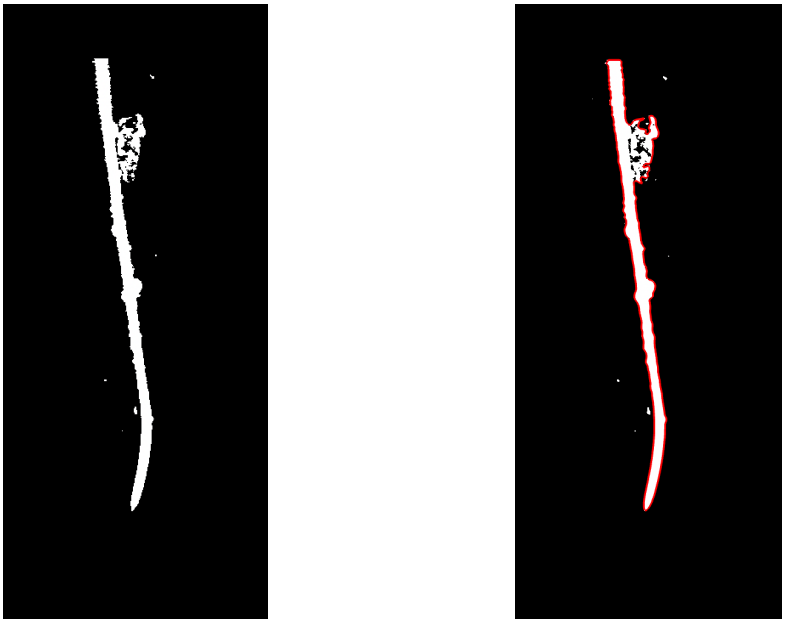

Figure 21: Distorted contour of a root surrounded by air or water bubbles extracted by KymoRod.

4. Discussion

To investigate the responses of root growth behaviour to local mechanical stress, a time-lapse imaging system in hydroponics was implemented. By combining this with kinematic analysis, it could be observed that primary roots did not react to an impairment of their seminal roots. A horizontal restriction of the primary and seminal root let the unimpeded roots grow shallower (chapter 3.2.1) and increased the seminal root growth rate (chapter 3.2.2). In contrast, a vertical restriction of the seminal root growth led to a change towards a steeper growth direction and a decrease in growth rate of the unimpeded root.

4.1 In-vivo quantification of root growth in hydroponics using time-lapse imaging and kinematics

The method was able to provide information about the complex movement processes in roots (Bastien et al. 2016). Using a hydroponic system, roots could get investigated without damaging the roots (Nguyen et al. 2016). The seeds pre-germinated in the nutrient solution and after transplanting, also grew in the growth container filled with the nutrient solution. This enabled an in vivo investigation in real-time (Nguyen et al. 2016). The time-lapse imaging then took pictures for 24 hours, which could be used by KymoRod to create velocity, elongation and curvature profiles (Bastien et al. 2016). Thereby, the root growth rate, the maximal elemental elongation rate, the length of the growth zone and the curvature could be quantified (Bizet et al. 2015). As already done in Youssef et al. 2018, this study could relate the root growth rate to its driving forces under optimal conditions and under local mechanical stress. Therefore, time-lapse imaging in hydroponics in combination with kinematics analysis, can be used to investigate the underlying processes of root growth.

Nevertheless, using the method for the first time caused challenges. The roots did not always show optimal growth. As always 10 seeds were pre-geminated at the same time, competition in space might have been occurred for the developing root system. This might have impaired or ceased the root growth at the zone of contact with the neighboring roots, which leads to an either lower performance of the root system (Brisson & Reynolds 194). Therefore, a reduction in to-germinating seeds might improve the root conditions. Moreover, sometimes the aeration in the system

was not ensured since the pumps were not properly inserted into the solution, which might have led to hypoxic conditions, which in turn might have affected root growth negatively (Drew 2013; Miro & Ismail 2013). However, root growth is a complex process (Tanimoto 2005; Su et al. 2017), which underlies natural variability (Ristova & Busch 2014). Therefore, the high seedling density and the lack of aeration might have only been one possible explanation for the differences in root growth behavior.

For the analysis, it is important that the root is in the field of view for at least the time span of 2 hours before and 4 hours after the reach of the obstacle. Therefore, an adjustment of the distance between the obstacle and the placement is necessary. To ensure an accurate analysis of the images, also the quality of the images is crucial, which in turn depends on the light intensity and the direction of illumination (Bastien et al. 2016). By illuminating the roots with a low incidence angle, natural marks on the root surface become visible. To what extend the light gets reflected might thereby depend on the different plant components such as the cell wall orientation and the cell density (Bizet et al. 2015). This led to the fact that depending on the angle the roots were illuminated, parts of the roots showed no illuminated natural marks, while noises (water bubbles, air bubbles and clue of the rubber band stacks) in the growth system became visible and therefore were included in the analysis. Therefore, adjusted light setting in combination with an adjusted obstacle distances and a more uniform initial root length, would enable a more reasonable analysis

4.2 Impact of local mechanical stress on root growth direction

The primary roots showed a generally steep growth, but no significant change in growth direction in response to the applied stress (Fig. 14A). This is in line with findings from Nakamoto (1994), where the excision of the first seminal root pair had no effect on the primary root but on the second pair of seminal roots. In contrast, the seminal roots responded slightly to the restricted growth rate of their neighboring roots with a change in growth direction (Fig. 14B). During the first hour, no bending could be observed, which is in line with Falik et al. (2012), who also observed a response to stress signals after 1 hour. After this first hour, it could be seen that the seminal roots whose neighboring roots were blocked horizontally did not compensate (Crossett et al. 1975; Robinson et al. 2013) with a steeper growth as it was shown in Nakamoto (1994), but slightly changed to a shallower root growth (Fig. 14B). However, a change towards a steeper growth can be observed for the roots, whose neighboring roots got restricted vertically (Fig. 14B). Hence, they also did not compensate for the restricted shallow growth of their

neighboring roots, but changed to the same direction, to which the restricted root had to evade. Therefore, it might be possible, that the roots react to the stress sensed and communicated by the other root, in the same way as the local mechanical stress would have occurred on their side.

The mechanism of responding to situations which have not yet occurred is already known for plants (Karban 2008). Thereby, plants not only react to cues which indicate future conditions (Karban 2008), but can respond to stress signals from other organs. In a study on split-root *Pisum sativum* L. plants, Falik et al (2012) found out that roots, which were exposed to osmotic stress or drought communicated their stress conditions to unstressed neighbor plants, which also reacted with a closure of the stomata even if the stress was not applied to them.
In previous studies, it could be shown, how the reaction to stress situations, which have not yet appeared, also occurs within the same plant. Leaves reacted to water stress signals from the roots with a reduced expansion rate, even if the leaves were kept turgid (Passioura 1988). In my study, it could now be shown, that the communication of local mechanical stress might also occur from one root to another within the same root system, which leads to a reaction even if the stress was not sensed by the root itself. This response of a change in growth direction of the seminal roots equaled out again during the last hour of analysis (Fig. 14B). This confirms the findings of Falik et al. (2012), which show that 3 to 24 hours after reacting to the stress signals, the plants normalize their behavior again as no real stress is sensed in their environment.
However, as in my experiment the results were not significant and only represent the growth behavior of 4 replicates, this explanation should be considered with caution.

4.3 Impact of local mechanical stress on root growth rate

As already seen for the growth direction, the primary root did not respond with a change in growth rate to the restricted root growth of their seminal roots. In contrast, the seminal roots again showed a reaction to the impairment of their neighboring roots (Fig. 15C and 15D). The contrasting responses of the primary and seminal roots might be caused by their different functions. which is why they react differently on different stresses (Morita & Abe 1994). The primary root grows to deeper layers to anker the plant and access water resources (Dardanelli et al. 2004; Lynch 2013; Bellini et al. 2014). Therefore, they do not compete for nutrients with the seminal roots. Since most of the nutrient uptake is done by the seminal roots, they can rather compensate for an impairment of nutrient uptake by the primary root than the other way around (Kirk 2003).

Therefore, the root growth rate of the other seminal root decreased compared to roots that were not exposed to mechanical stress in response to a vertical impedance of the other seminal root (Fig. 15D). As already discussed for the growth direction, this shows that the root reacts to the stress, which is applied to their neighboring root (Passioura 1988; Falik et al. 2012) in the same manner as the impaired root does, hence by a decrease in their natural growth rate.

Nevertheless, if the seminal root was restricted horizontally, the second seminal root grew significantly faster and reached even higher relative growth rates than the roots which grew under optimal conditions (Fig. 15D). The fact, that the roots reacted differently to a horizontal than to a vertical restriction might be explained by their natural growth direction. Seminal roots are characterized by a shallow, plagiotropic growth to spread in the topsoil (Morita & Abe 1994; Nakamoto & Oyanagi 1994; Lynch 2013). Therefore, the root can react to the applied stress of the other root with a change towards a more pronounced shallow growth as discussed in the previous chapter. Having the opportunity to work around the anticipated stress without a limitation in function, the root then tries to compensate for the restricted root growth of the other roots (Crossett et al. 1975). Here, the root which is not restricted might be promoted by getting more growth substances (Nakamoto & Oyanagi 1994), as plants invest in parts where the returns equalize the investments (Maina et al. 2002).

Similar to the change in growth direction and the results of Falik et al. (2012), the increase in growth rate and therefore the response to the local mechanical stress occurred within a time span of one hour (Fig. 15D). In contrast to the growth direction, which equaled out after the anticipated stress could not be sensed, the increase in growth rate of the compensating roots continued. This supports the results of previous studies investigating compensatory growth, where the compensatory effect was maintained for the whole growth period (Wightman et al. 1980; Nakamoto & Oyanagi 1994). In further research it would be interesting to see if a vertical impairment can also lead to a compensatory growth of the other root after sensing no stress on their side. To answer this question, an analysis of growth periods longer than 4 hours would be necessary.

4.4 Drivers of growth rate

In this study, all roots of the control treatment increased their growth rate constantly over the whole period of analysis (Fig. 15), which confirms that roots grow linearly (Youssef et al. 2018). Looking at the drivers for the growth rate, results were not entirely consistent with literature. Previous studies show, that the growth zone length and the cell elongation rate represent the main drivers of growth rate (Baskin 2013). For the primary roots, this study could confirm that the length of the growth

zone is a good predictor for the growth rate (Baskin 2013). Here, the relative growth rate followed the same pattern as the relative length of the growth zone (Fig. 15C and 16C), respectively a general tendency towards a faster growth rate and a longer growth zone over time. This could not be observed for the seminal roots. Here, the relative length of the growth zone increased over time, but so did not the relative growth length (Fig 15D and 17D).

However, in previous studies, it could be shown, that along the growth zone, the cell elongation rate is the main driver for the growth rate (Silk 1992), which mainly takes place in the elongation zone of the root apex (Bizet et al. 2015). Therefore, Youssef et al. (2018) defined the length of the elongation zone as the best proxy for the growth rate as it summarizes the cell production rate in the root apical meristem and the cell elongation rate in one parameter.

In this study, this could not be confirmed for the primary roots, as the relative elemental elongation rate, which served as a proxy for the cell elongation rate, followed a different pattern than the relative growth rate (Fig. 15C and 16C). In contrast, it could be seen, that for the seminal roots, the relative elemental elongation rate and the relative growth rate followed the same trend (Fig. 15D and 16D). An increase of the relative growth rate correlated with an increase of the relative elemental elongation rate, while it decreased at the same time when also the relative growth rate decreased. The fact, that the elemental elongation rate was stronger associated with the growth rate for the seminal roots, which showed a response to the applied stress, corresponds with the findings of Youssef et al. (2018) which show that the elemental elongation rate is the main driver for short-term adjustments. As the differences between the treatments were not significant, more replicates and adjustments of the method might increase the quality of the results and therefore also provide better information about the correlation between the different parameters.

5. Conclusion and outlook

In this study, the underlying processes of root growth were analysed by doing time-lapse imaging in a hydroponic system in combination with particle image velocimetry in KymoRod. The analysis showed that primary roots do not react to a restriction of their neighbouring roots with a change in growth behaviour. This can be explained by the fact, that primary roots have different functions and reach out to different layers than seminal roots.

Against my expectations, the seminal roots did not compensate with a change in growth direction for the restricted root growth of their neighbouring roots but changed to the same direction. Therefore, it might be possible, that they anticipate the same stress in their surroundings. After 3 hours, this response equalled out as no stress could be recognised. In cases, where the root bent away from its natural shallow growth direction, also the growth rate decreased. When the neighbouring root got restricted horizontally, roots intensified its shallow growth direction. Finding a way to work around the anticipated stress, the roots then started to compensate for the impeded root by an increased growth rate. The driving forces of these adjusted growth rates of the seminal roots might be the elemental elongation rate, while the length of the growth zone might be the driver when roots do not react to stresses.

Verifying these results by adjusting the method and including more replicates will provide important information about root responses to local mechanical stress. In further research, it might be interesting to include a second genotype. Different genotypes differ in their root alignment according to the soil conditions (McKenzie et al. 2009) and their behavior in root bending (Qi & Zheng 2013), as well as in their tolerance to drought and mechanical stress. Therefore, including more genotypes in the experiment might provide information about if responses to local mechanical stress differ for different genotypes. This would enable an establishment of root systems which are best adapted to spatial variability in soils. Further research could also give more insights into which genes and hormones are involved in transferring and responding to the applied stress.

References

Adrian, R.J. & Westerweel, J. (2011). *Particle Image Velocimetry*. Cambridge University Press.

Atkinson, J.A., Hawkesford, M.J., Whalley, W.R., Zhou, H. & Mooney, S.J. (2020). Soil strength influences wheat root interactions with soil macropores. *Plant, Cell & Environment*, 43 (1), 235–245. https://doi.org/10.1111/pce.13659

Barley, K.P. (1970). The Configuration of the Root System in Relation to Nutrient Uptake. *Advances in Agronomy*. Elsevier, 159–201. https://doi.org/10.1016/S0065-2113(08)60268-0

Baskin, T.I. (2013). Patterns of root growth acclimation: constant processes, changing boundaries: Patterns of root growth acclimation. *Wiley Interdisciplinary Reviews: Developmental Biology*, 2 (1), 65–73. https://doi.org/10.1002/wdev.94

Bastien, R., Legland, D., Martin, M., Fregosi, L., Peaucelle, A., Douady, S., Moulia, B. & Höfte, H. (2016). KymoRod: a method for automated kinematic analysis of rod-shaped plant organs. *The Plant Journal*, 88 (3), 468–475. https://doi.org/10.1111/tpj.13255

Beemster, G.T.S. & Baskin, T.I. (1998). Analysis of Cell Division and Elongation Underlying the Developmental Acceleration of Root Growth in Arabidopsis thaliana1. *Plant Physiology*, 116 (4), 1515–1526. https://doi.org/10.1104/pp.116.4.1515

Bellini, C., Pacurar, D.I. & Perrone, I. (2014). Adventitious Roots and Lateral Roots: Similarities and Differences. *Annual Review of Plant Biology*, 65 (1), 639–666. https://doi.org/10.1146/annurev-arplant-050213-035645

Bengough, A.G., Bransby, M.F., Hans, J., McKenna, S.J., Roberts, T.J. & Valentine, T.A. (2006). Root responses to soil physical conditions; growth dynamics from field to cell. *Journal of Experimental Botany*, 57 (2), 437–447. https://doi.org/10.1093/jxb/erj003

Bengtsson, Henrik, et al. "Package 'R. matlab'." (2018).

Bizet, F., Bengough, A.G., Hummel, I., Bogeat-Triboulot, M.-B. & Dupuy, L.X. (2016). 3D deformation field in growing plant roots reveals both mechanical and biological responses to axial mechanical forces. *Journal of Experimental Botany*, 67 (19), 5605–5614. https://doi.org/10.1093/jxb/erw320

Bizet, F., Hummel, I. & Bogeat-Triboulot, M.-B. (2015). Length and activity of the root apical meristem revealed in vivo by infrared imaging. *Journal of Experimental Botany*, 66 (5), 1387–1395. https://doi.org/10.1093/jxb/eru488

Bray, R.H. (1953). A nutrient mobility concept of soil-plant relationships. *Soil Sci.* 78, 9-22.

Brisson, J. & Reynolds, J.F. (1994). The Effect of Neighbors on Root Distribution in a Creosotebush (Larrea Tridentata) Population. *Ecology*, 75 (6), 1693–1702. https://doi.org/10.2307/1939629

Chen, R., Rosen, E. & Masson, P.H. (1999). Gravitropism in Higher Plants1. *Plant Physiology*, 120 (2), 343–350. https://doi.org/10.1104/pp.120.2.343

Clark, L.J., Whalley, W.R. & Barraclough, P.B. (2003). How do roots penetrate strong soil? 12

Clément, R., Douady, S. & Mauroy, B. (2012). Branching geometry induced by lung self-regulated growth. *Physical Biology*, 9 (6), 066006. https://doi.org/10.1088/1478-3975/9/6/066006

Conn, S.J., Hocking, B., Dayod, M., Xu, B., Athman, A., Henderson, S., Aukett, L., Conn, V., Shearer, M.K., Fuentes, S., Tyerman, S.D. & Gilliham, M. (2013). Protocol: optimising hydroponic growth systems for nutritional and physiological analysis of Arabidopsis thaliana and other plants. *Plant Methods*, 9 (1), 4. https://doi.org/10.1186/1746-4811-9-4

Correa, J., Postma, J.A., Watt, M. & Wojciechowski, T. (2019). Soil compaction and the architectural plasticity of root systems. (Zhang, J., ed.) *Journal of Experimental Botany*, 70 (21), 6019–6034. https://doi.org/10.1093/jxb/erz383

Crossett, R.N., Campbell, D.J. & Stewart, H.E. (1975). Compensatory growth in cereal root systems. *Plant and Soil*, 42 (3), 673–683. https://doi.org/10.1007/BF00009951

Dardanelli, J.L., Ritchie, J.T., Calmon, M., Andriani, J.M. & Collino, D.J. (2004). An empirical model for root water uptake. *Field Crops Research*, 87 (1), 59–71. https://doi.org/10.1016/j.fcr.2003.09.008

Drew, M.C. (2013). Plant responses to anaerobic conditions in soil and solution culture. *Commentaries in Plant Science*.

de Mendiburu, Felipe. "Tutorial de agricolae (Versión 1.2-8)." (2017).

Falik, O., Mordoch, Y., Ben-Natan, D., Vanunu, M., Goldstein, O. & Novoplansky, A. (2012). Plant responsiveness to root–root communication of stress cues. *Annals of Botany*, 110 (2), 271–280. https://doi.org/10.1093/aob/mcs045

Forterre, Y. (2013). Slow, fast and furious: understanding the physics of plant movements. *Journal of Experimental Botany*, 64 (15), 4745–4760. https://doi.org/10.1093/jxb/ert230

He, Y.B., Lin, L.R. & Chen, J.Z. (2017). Maize root morphology responses to soil penetration resistance related to tillage and drought in a clayey soil. *The Journal of Agricultural Science*, 155 (7), 1137–1149. https://doi.org/10.1017/S0021859617000302

Hodge, A., Berta, G., Doussan, C., Merchan, F. & Crespi, M. (2009). Plant root growth, architecture and function. *Plant and Soil*, 321 (1–2), 153–187. https://doi.org/10.1007/s11104-009-9929-9

Ingram, K.T. & Leers, G.A. (2001). Software for Measuring Root Characters from Digital Images. *Agronomy Journal*, 93 (4), 918–922. https://doi.org/10.2134/agronj2001.934918x

Jabro, J.D., Iversen, W.M., Evans, R.G., Allen, B.L. & Stevens, W.B. (2014). Repeated Freeze-Thaw Cycle Effects on Soil Compaction in a Clay Loam in Northeastern Montana. *Soil Science Society of America Journal*, 78 (3), 737–744. https://doi.org/10.2136/sssaj2013.07.0280

Jiang, K. & Feldman, L.J. (2005). REGULATION OF ROOT APICAL MERISTEM DEVELOPMENT. *Annual Review of Cell and Developmental Biology*, 21 (1), 485–509. https://doi.org/10.1146/annurev.cellbio.21.122303.114753

Jin, K., Shen, J., Ashton, R.W., Dodd, I.C., Parry, M.A.J. & Whalley, W.R. (2013). How do roots elongate in a structured soil? *Journal of Experimental Botany*, 64 (15), 4761–4777. https://doi.org/10.1093/jxb/ert286

Jin, W., Aufrecht, J., Patino-Ramirez, F., Cabral, H., Arson, C. & Retterer, S.T. (2020). Modeling root system growth around obstacles. *Scientific Reports*, 10 (1), 15868. https://doi.org/10.1038/s41598-020-72557-8

Karban, R. (2008). Plant behaviour and communication. *Ecology Letters*, 11 (7), 727–739. https://doi.org/10.1111/j.1461-0248.2008.01183.x

Kirk, G.J.D. (2003). Rice root properties for internal aeration and efficient nutrient acquisition in submerged soil. *New Phytologist*, 159 (1), 185–194. https://doi.org/10.1046/j.1469-8137.2003.00793.x

Koebernick, N., Daly, K.R., Keyes, S.D., George, T.S., Brown, L.K., Raffan, A., Cooper, L.J., Naveed, M., Bengough, A.G., Sinclair, I., Hallett, P.D. & Roose, T. (2017). High-resolution synchrotron imaging shows that root hairs influence rhizosphere soil structure formation. *New Phytologist*, 216 (1), 124–135. https://doi.org/10.1111/nph.14705

Koevoets, I.T., Venema, J.H., Elzenga, J.Theo.M. & Testerink, C. (2016). Roots Withstanding their Environment: Exploiting Root System Architecture Responses to Abiotic Stress to Improve Crop Tolerance. *Frontiers in Plant Science*, 07. https://doi.org/10.3389/fpls.2016.01335

Kopittke, P.M., Blamey, F.P.C., Asher, C.J. & Menzies, N.W. (2010). Trace metal phytotoxicity in solution culture: a review. *Journal of Experimental Botany*, 61 (4), 945–954. https://doi.org/10.1093/jxb/erp385

Lipiec, J., Kuś, J., Słowińska-Jurkiewicz, A. & Nosalewicz, A. (2006). Soil porosity and water infiltration as influenced by tillage methods. *Soil and Tillage Research*, 89 (2), 210–220. https://doi.org/10.1016/j.still.2005.07.012

Lynch, J.P. (2013). Steep, cheap and deep: an ideotype to optimize water and N acquisition by maize root systems. *Annals of Botany*, 112 (2), 347–357. https://doi.org/10.1093/aob/mcs293

Maina, G.G., Brown, J.S. & Gersani, M. (2002). Intra-plant versus Inter-plant Root Competition in Beans: avoidance, resource matching or tragedy of the commons. 13

Martino, D.L. & Shaykewich, C.F. (1994). Root penetration profiles of wheat and barley as affected by soil penetration resistance in field conditions. *Canadian Journal of Soil Science*, 74 (2), 193–200. https://doi.org/10.4141/cjss94-027

McKenzie, B.M., Bengough, A.G., Hallett, P.D., Thomas, W.T.B., Forster, B. & McNicol, J.W. (2009). Deep rooting and drought screening of cereal crops: A novel field-based method and its application. *Field Crops Research*, 112 (2–3), 165–171. https://doi.org/10.1016/j.fcr.2009.02.012

Melnyk, C.W. (2017). Connecting the plant vasculature to friend or foe. *New Phytologist*, 213 (4), 1611–1617. https://doi.org/10.1111/nph.14218

Miro, B. & Ismail, A.M. (2013). Tolerance of anaerobic conditions caused by flooding during germination and early growth in rice (Oryza sativa L.). *Frontiers in Plant Science*, 4. https://doi.org/10.3389/fpls.2013.00269

Monshausen, G.B. & Gilroy, S. (2009). The exploring root—root growth responses to local environmental conditions. *Current Opinion in Plant Biology*, 12 (6), 766–772. https://doi.org/10.1016/j.pbi.2009.08.002

Morita, S. & Abe, P. (1994). Development of Root Systems in Wheat and Rice. *Roots and Nitrogen in Cropping Systems*. 185–198

Moulia, B. (2013). Plant biomechanics and mechanobiology are convergent paths to flourishing interdisciplinary research. *Journal of Experimental Botany*, 64 (15), 4617–4633. https://doi.org/10.1093/jxb/ert320

Muthert, L.W.F., Izzo, L.G., van Zanten, M. & Aronne, G. (2020). Root Tropisms: Investigations on Earth and in Space to Unravel Plant Growth Direction. *Frontiers in Plant Science*, 10, 1807. https://doi.org/10.3389/fpls.2019.01807

Nakamoto, T. & Oyanagi, A. (1994). The Direction of Growth of Seminal Roots of Triticum aestivum L. and Experimental Modification Thereof. *Annals of Botany*, 73 (4), 363–367. https://doi.org/10.1006/anbo.1994.1045

Neuwirth, Erich, and Maintainer Erich Neuwirth. "Package 'RColorBrewer'." ColorBrewer Palettes (2014).

Nguyen, N.T., McInturf, S.A. & Mendoza-Cózatl, D.G. (2016). Hydroponics: A Versatile System to Study Nutrient Allocation and Plant Responses to Nutrient Availability and Exposure to Toxic Elements. *Journal of Visualized Experiments*, (113), 54317. https://doi.org/10.3791/54317

Passioura, J. (1988). Root Signals Control Leaf Expansion in Wheat Seedlings Growing in Drying Soil. *Functional Plant Biology*, 15 (5), 687. https://doi.org/10.1071/PP9880687

Petricka, J.J., Winter, C.M. & Benfey, P.N. (2012). Control of *Arabidopsis* Root Development. *Annual Review of Plant Biology*, 63 (1), 563–590. https://doi.org/10.1146/annurev-arplant-042811-105501

Pflugfelder, D., Kochs, J., Koller, R., Jahnke, S., Mohl, C., Pariyar, S., Fassbender, H., Nagel, K.A., Watt, M. & van Dusschoten, D. (2021). The root system architecture of wheat establishing in soil is associated with varying elongation rates of seminal roots: quantification using 4D magnetic resonance imaging. (Takahashi, H., ed.) *Journal of Experimental Botany*, erab551. https://doi.org/10.1093/jxb/erab551

Pinheiro, José, et al. "Package 'nlme'." Linear and nonlinear mixed effects models, version 3.1 (2017).

Py, C., de Langre, E., Moulia, B. & Hémon, P. (2005). Measurement of wind-induced motion of crop canopies from digital video images. *Agricultural and Forest Meteorology*, 130 (3–4), 223–236. https://doi.org/10.1016/j.agrformet.2005.03.008

Qi, B. & Zheng, H. (2013). Modulation of root-skewing responses by KNAT1 in Arabidopsis thaliana. *The Plant Journal*, 76 (3), 380–392. https://doi.org/10.1111/tpj.12295

Rillig, M.C. & Mummey, D.L. (2006). Mycorrhizas and soil structure. *New Phytologist*, 171 (1), 41–53. https://doi.org/10.1111/j.1469-8137.2006.01750.x

Ristova, D. & Busch, W. (2014). Natural Variation of Root Traits: From Development to Nutrient Uptake. *PLANT PHYSIOLOGY*, 166 (2), 518–527. https://doi.org/10.1104/pp.114.244749

Robinson, D. (1997). Variation, co-ordination and compensation in root systems in relation to soil variability. In: Anderson, H.M., Barlow, P.W., Clarkson, D.T., Jackson, M.B., & Shewry, P.R. (eds.) *Plant Roots - From Cells to Systems: Proceedings of the 14th Long Ashton International Symposium Plant Roots — From Cells to Systems, held in Bristol, U.K., 13–15 September 1995*. Dordrecht: Springer Netherlands, 57–66. https://doi.org/10.1007/978-94-011-5696-7_6

Robinson, S., Burian, A., Couturier, E., Landrein, B., Louveaux, M., Neumann, E.D., Peaucelle, A., Weber, A. & Nakayama, N. (2013). Mechanical control of morphogenesis at the shoot apex. *Journal of Experimental Botany*, 64 (15), 4729–4744. https://doi.org/10.1093/jxb/ert199

Sauer, T.J. & Logsdon, S.D. (2002). Hydraulic and Physical Properties of Stony Soils in a Small Watershed. *Soil Science Society of America Journal*, 66 (6), 1947–1956. https://doi.org/10.2136/sssaj2002.1947

Sharp, R.E., Silk, W.K. & HsIAO, T.C. (1988). I. SPATIAL DISTRIBUTION OF EXPANSIVE GROWTH. 87, 8

Silk, W.K. (1992). Steady Form from Changing Cells. *International Journal of Plant Sciences*, 153 (3, Part 2), S49–S58. https://doi.org/10.1086/297063

Su, S.-H., Gibbs, N.M., Jancewicz, A.L. & Masson, P.H. (2017). Molecular Mechanisms of Root Gravitropism. *Current Biology*, 27 (17), R964–R972. https://doi.org/10.1016/j.cub.2017.07.015

Tanimoto, E. (2005). Regulation of Root Growth by Plant Hormones—Roles for Auxin and Gibberellin. *Critical Reviews in Plant Sciences*, 24 (4), 249–265. https://doi.org/10.1080/07352680500196108

Voroney, R.P. (2007). THE SOIL HABITAT. *Soil Microbiology, Ecology and Biochemistry*. Elsevier, 25–49. https://doi.org/10.1016/B978-0-08-047514-1.50006-8

Waisel, Y., Eshel, A., Beeckman, T. & Kafkafi, U. (2002). *Plant Roots: The Hidden Half, Third Edition*. CRC Press.

Wang, X., Whalley, W.R., Miller, A.J., & White (2020). Sustainable Cropping Requires Adaptation to a Heterogeneous Rhizosphere. *2020*

Wightman, F., Schneider, E.A. & Thimann, K.V. (1980). Hormonal factors controlling the initiation and development of lateral roots. II. Effects of exogenous growth factors on lateral root formation in pea roots. *Physiologia Plantarum*, 49 (3), 304–314. https://doi.org/10.1111/j.1399-3054.1980.tb02669.x

Yamaguchi, M., Valliyodan, B., Zhang, J., Lenoble, M.E., Yu, O., Rogers, E.E., Nguyen, H.T. & Sharp, R.E. (2010). Regulation of growth response to water stress in the soybean primary root. I. Proteomic analysis reveals region-specific regulation of phenylpropanoid metabolism and control of free iron in the elongation zone. *Plant, Cell & Environment*, 33 (2), 223–243. https://doi.org/10.1111/j.1365-3040.2009.02073.x

Yamauchi, A., Pardales Jr, J.R. & Kono, Y. (1996). Root System Structure and Its Relation to Stress Tolerance. *Roots and Nitrogen in Cropping Systems of the Semi-Arid Tropics*.

Youssef, C., Bizet, F., Bastien, R., Legland, D., Bogeat-Triboulot, M.-B. & Hummel, I. (2018). Quantitative dissection of variations in root growth rate: a matter of cell proliferation or of cell expansion? *Journal of Experimental Botany*, 69 (21), 5157–5168. https://doi.org/10.1093/jxb/ery272

in t'Zandt, D., Le Marié, C., Kirchgessner, N., Visser, E.J.W. & Hund, A. (2015). High-resolution quantification of root dynamics in split-nutrient rhizoslides reveals rapid and strong proliferation of maize roots in response to local high nitrogen. *Journal of Experimental Botany*, 66 (18), 5507–5517. https://doi.org/10.1093/jxb/erv307

Popular science summary

Roots play an important role for the plant growth and productivity. By taking up nutrients from the soil, they provide the plant with important resources. Thereby, it is not only important that different nutrients and water are available, but they also need to be accessible. To reach the different nutrients and water, an optimal root growth is needed. As roots grow in soil, roots growth is influenced by their surrounding soil conditions positively and negatively. While a well-structured soil stimulates root growth to the different resources, hard and dry soils with large aggregates or stones increase the penetration resistance and impede the root growth. Due to different climate and bedrock conditions, different agricultural management practices and complex soil processes, the soil varies spatially, even on a small scale. Therefore, the different roots of a single root system can be exposed to different soil conditions. Since the roots are connected by their cell walls, they can exchange information and by this, react on the conditions of their neighbouring roots.

In this study, a hydroponic system was used in combination with a time-lapse imaging system and particle image velocimetry to study the root response of an unimpeded root to a restricted root growth of another root in the root system. Using kinematic analysis, the underlying processes of a change in root growth, such as the growth rate, the elemental elongation rate, the length of the growth zone and the curvature were investigated in response to an impairment of another root.

To do so, roots were grown for 24 hours in a nutrient solution. Thereby, either the seminal or the primary root was exposed to a vertical or horizontal obstacle. All treatments were also compared to roots which were not impeded. Time-lapse images were taken under infra-red light over the 24 hours, which were then analysed in the software KymoRod.

It could be shown that primary roots and seminal roots did respond differently to the applied stress. Primary roots did not react to an impeded root growth of the seminal roots. This might be due to the fact, that primary roots are responsible for different functions in the root system and grow into different regions of the soil, which is why they do not compete with the seminal roots. In contrast, did the treatments influence the growth direction and the growth rate of the seminal roots. Seminal roots showed the same change in growth direction as the impeded roots. They changed to a shallower growth when their neighbouring root was restricted horizontally, while they grew steeper if the other root was exposed to a vertical

obstacle. This might be because they anticipate the same growth impairment as the other root realizes. Three hours after the root reached the obstacle, the change in growth direction of the other root equalled out, as they might have realized that no stress occurred in their growth region. In the cases where the seminal root got restricted vertically, which implicates a restriction in their natural growth direction, the other seminal root responded with a decreased growth rate. Again here, the restriction of the other root might be anticipated. However, if the roots were restricted horizontally the other root might have still anticipated the stress but worked around it by reinforcing its shallow growth direction. Here, they started to increase their growth rate to compensate for the restricted seminal root. The driving forces of the growth rate might be the length of the growth zone, when the roots do not react to stresses, while the elemental elongation rate might be the driver for adjustments of the growth rate.

Further investigation with more replicates and an adjustment of light settings, transplanting position, and growth conditions is needed to confirm the observed trends and gain information about root responses to local mechanical stress. Furthermore, the inclusion of a second genotype might provide information on if the response to local mechanical stress of non-impeded roots is determined genetically. This would allow the establishment of root systems best adapted to soil heterogeneities.

Acknowledgements

I would like to thank my main supervisor Dr. Tino Colombi for outstanding supervision, for his attention and patience and for being available at all times. I would also like to thank Daniel Iseskog for making the experiment possible and for allowing me to contact him with technical questions and Mina Spångberg, who was always super friendly helping with questions about the laboratory. Further thanks go to my co-supervisor Dr Thomas Keller and the entire Soil Mechanics and Soil Management research group for their welcoming supportive nature and feedback in the team meetings. Finally, I would like to thank Anna Lackner for her opposition and all the other Master students who made the time at the institute enjoyable.

Appendix 1

Table S 1: Runs which were taken into the analysis and their tresholds chosen manually in Kymorod.

Treatment	Run	Roots	Treshold KymoRod
Control	Run 1	Left seminal	52
		Right seminal	36
		Primary	32
	Run 31	Left seminal	28
		Right seminal	30
		Primary	34
	Run 43	Left seminal	36
		Right seminal	48
		Primary	36
	Run 46	Left seminal	46
		Right seminal	38
		Primary	28
Primary horizontal	Run 3	Left seminal	44
		Right seminal	46
	Run 14	Left seminal	40
		Right seminal	42
	Run 21	Left seminal	32
		Right seminal	26
	Run 48	Left seminal	28
		Right seminal	38
Seminal vertical	Run 11	Left seminal	44
		Primary	46
	Run 16	Left seminal	52
		Primary	24
	Run 20	Left seminal	32
		Primary	28
	Run 39	Left seminal	52
		Primary	42

	Run 2	Left seminal	42
		Primary	30
	Run 15	Left seminal	48
		Primary	36
Seminal horizontal	Run 41	Left seminal	42
		Primary	32
	Run 47	Left seminal	42
		Primary	48

Table S 2: Germination time, transplanting time and the primary root length of the chosen runs.

Run	**Germination time**	**Transplanting time**	**Primary root length**
Run 1	01.02.2022, 17h	04.02.2022, 8h	2.4 cm
Run 2	04.02.2022, 17h	07.02.2022, 8h	2.4 cm
Run 3	07.02.2022, 17h	10.02.2022, 8h	2.7 cm
Run 11	28.02.2022, 17h	03.03.2022, 8h	2.4 cm
Run 14	07.03.2022, 8h	09.03.2022, 17h	2.7 cm
Run 15	08.03.2022, 8h	10.03.2022, 17h	2.4 cm
Run 16	09.03.2022, 8h	11.03.2022, 17h	2.1 cm
Run 20	16.03.2022, 8h	18.03.2022, 17h	1.9 cm
Run 21	18.03.2022, 17h	21.03.2022, 8h	2.6 cm
Run 31	04.04.2022, 8h	06.04.2022, 17h	2.8 cm
Run 39	13.04.2022, 8h	15.04.2022, 17h	2.2 cm
Run 41	15.04.2022, 17h	18.04.2022, 8h	2 cm
Run 43	19.04.2022, 8h	21.04.2022, 17h	2.4 cm
Run 46	22.04.2022, 17h	25.04.2022, 8h	2.8 cm
Run 47	25.04.2022, 8h	27.04.2022, 17h	2.2 cm
Run 48	26.04.2022, 8h	28.04.2022, 17h	2.4 cm

Table S 3: Images of the different runs, which were analyzed in KymoRod.

Run	**Treatment**	**Images taken into the analysis**
Run 1	Control	228-408
Run 2	Seminal horizontal	140-320
Run 3	Primary horizontal	384-564
Run 11	Seminal vertical	454-614
Run 14	Primary horizontal	220-400
Run 15	Seminal horizontal	80-260
Run 16	Seminal vertical	218-398
Run 20	Seminal vertical	1092-1272
Run 21	Primary horizontal	541-721
Run 31	Control	232-412
Run 39	Seminal vertical	830-1070
Run 41	Seminal horizontal	100-280
Run 43	Control	228-408
Run 46	Control	228-408
Run 47	Seminal horizontal	97-274
Run 48	Primary horizontal	190-370

Table S 4 Settings for the automated image analysis in Kymorod.

Setting	**Setting**
Image file pattern	*tif
Color images channel	Red
Spatial Resolution	8.8 µm
Time interval	2 min
Frame selection	Keep all frames
Method	Box Filter
Threshold	Manual threshold
Contour Smoothing factor	20
Curvature smoothing	150
Number of points for resampling	500
First point of Skeleton	bottom
Channel for displacement	Red
Step between two measurements of displacement	2
Size of correlating window	20
Spatial Smoothing	0.4
Value Smoothing	0.02
Resampling distance	0.005
Size of derivation window	20

Publishing and archiving

Approved students' theses at SLU are published electronically. As a student, you have the copyright to your own work and need to approve the electronic publishing. If you check the box for **YES**, the full text (pdf file) and metadata will be visible and searchable online. If you check the box for **NO**, only the metadata and the abstract will be visible and searchable online. Nevertheless, when the document is uploaded it will still be archived as a digital file. If you are more than one author, the checked box will be applied to all authors. Read about SLU's publishing agreement here:

☒ YES, I/we hereby give permission to publish the present thesis in accordance with the SLU agreement regarding the transfer of the right to publish a work.

☐ NO, I/we do not give permission to publish the present work. The work will still be archived and its metadata and abstract will be visible and searchable.